ERDC/GSL TR-01-8

US Army Corps
of Engineers®
Engineer Research and
Development Center

Convex Watershed-Reservoir Model for Risk Assessment of Spillways and Nonoverflow Dam Monoliths Subjected to Flood Hazard

Luis A. de Béjar

August 2001

Geotechnical and Structures Laboratory

The contents of this report are not to be used for advertising, publication, or promotional purposes. Citation of trade names does not constitute an official endorsement or approval of the use of such commercial products.

The findings of this report are not to be construed as an official Department of the Army position, unless so designated by other authorized documents.

PRINTED ON RECYCLED PAPER

ERDC/GSL TR-01-8
August 2001

Convex Watershed-Reservoir Model for Risk Assessment of Spillways and Nonoverflow Dam Monoliths Subjected to Flood Hazard

by Luis A. de Béjar

Geotechnical and Structures Laboratory
U.S. Army Engineer Research and Development Center
3909 Halls Ferry Road
Vicksburg, MS 39180-6199

Final report

Prepared for U.S. Army Corps of Engineers
Washington, DC 20314-1000

Contents

List of Figures

Preface

This investigation introduces a convex model to describe the response of watershed-reservoir-dam systems to water-input events and to build corresponding flood hazard curves in support of evaluations of risk for dam safety. The work was funded by Headquarters, Department of the Army, under the Civil Works Research and Development Program.

Dr. Luis A. de Béjar, Geotechnical and Structures Laboratory (GSL), Geosciences and Structures Division, Structural Mechanics Branch, ERDC, was Principal Investigator, performed the work, and prepared this report. The work was performed in GSL under the general supervision of Dr. Michael J. O'Connor, Director; Dr. David W. Pittman, Assistant Director; Dr. Mary E. Hynes, Technical Director for Civil Works; Dr. Robert L. Hall, Division Chief; and Mr. Frank D. Dallriva, Branch Chief. The work was coordinated at ERDC by Mr. Harvey H. Jones, Division Chief, Information Technology Laboratory.

The author gratefully acknowledges the support and guidance provided by the Office of the Chief of Engineers and by the multiple U.S. Army Engineer District representatives involved in the Field Review Group, Operations and Maintenance.

At the time of publication of this report, Director of ERDC was Dr. James R. Houston. Commander and Executive Director was COL John W. Morris III, EN.

Conversion Factors, Non-SI to SI Units of Measurement

Non-SI units of measurement used in this report can be converted to SI units as follows:

Multiply	By	To Obtain
Cubic feet	0.028	Cubic meters
Feet	0.3048	Meters
Inches	2.54	Centimeters
Kilosecond-feet	28.32	Cubic meters per second
Miles	1,609.0	Meters
Square miles	2.59	Square kilometers

1 Introduction

A realistic mathematical model for a watershed-reservoir-dam system should involve some inherently random components leading to a probabilistic representation. A closed-form solution for the response of the system to a given water-input event proves difficult to obtain, if not impossible, in view of the complexity and ultimate nonlinearity of the governing formulations. Consequently, to arrive at useful conclusions in the study of a given system, the analyst must conduct a large number of numerical simulations of possible realizations. For this procedure to be practical in exercises of risk assessment of spillways and dam nonoverflow monoliths under flood hazard, the associated mathematical model must be effective and economical. This report introduces a new engineering model for flood-risk analysis of watershed-reservoir-dam systems designed for application in multiple mathematical simulations while capturing the essential characteristics of the physical system.

Hyetographs for a given basin are built by inserting rational elements into the current state of practice (U.S. Bureau of Reclamation (USBR) 1976, 1977). A simplified representation of the watershed is introduced at the level of the fundamental unitgraph. All subsequent compositions are mathematically rigorous, leading to a convolution integral for a rational watershed-output hydrograph. The reservoir is represented by a nonlinear ordinary differential equation formulated on the basis of the principle of continuity and on the assumption of a convex reservoir. The spillway discharge is modeled using the von Mises semiempirical expression for a wide-weir flow (Street, Walters, and Vennard 1996). Deterministic interpretations of the model provide insight into physical behavior through parametric studies on the occurrence of hydrograph peaks, response spectra, and residual reservoir pools. Stochastic interpretations of the model provide insight into the resulting response random processes and the associated hazard curves necessary for subsequent evaluations of the probabilities of overtopping, overstressing, overturning, and sliding failures (Ellingwood 1995, de Béjar 1999).

The relevant features of the USBR recommended practical procedure are retained in the model. Soil Conservation Service (Miller and Clark 1960) maps of probable maximum precipitation (PMP) during extreme storms are adopted as mean values of extreme-value distributions. USBR empirical factors for the determination of excess rain are directly implemented as are the Soil Conservation Service (SCS) charts for cover-and-land-use complex coefficients.

To focus on the effect of a few essential factors on the system response and to keep the formulation sufficiently simple to promote physical insight, only the basic random variables are included in the watershed stochastic model: (a) storm magnitude and (b) watershed characteristic centroidal lag time. The study of the random process representing the variation in reservoir-pool in response to the water-input event is conducted with and without the presence of noise in the reservoir, for mutual comparison among the resulting hazard curves.

2 Analytical Models

The physical system to be modeled consists of three major components (Figure 1): the watershed or drainage basin, the reservoir or excess-rain storage, and the spillway-dam structure, generally equipped with a gate system for flood control and evacuation.

The U.S. Weather Bureau in collaboration with the U.S. Army Corps of Engineers have developed empirical charts to estimate the 6-hr, 10-square-mile PMP as the result of a uniform storm on such 'a point' within the basin area (USBR 1976, 1977). The proper chart to be applied depends on the specific geographical location of the project site. The charts are built for U.S. zones either east or west of the 105° meridian. To be specific, the model developed here applies to U.S. watersheds east of the 105° meridian, but a parallel development may just as easily be formulated for U.S. western watersheds.

Subsequently, the point-storm PMP is scaled up on the basis of empirical charts for the size of the specific drainage area under consideration and for several values of storm duration to estimate upper bounds of cumulative total rain falling uniformly over the watershed. These estimates of precipitation are taken as the known PMP distribution in time in the deterministic formulations, or as mean values of the extreme-value distribution of the largest values, type I (Gumbel distribution) in the probabilistic formulations.

The watershed represents the first filter in the system. A substantial portion of the falling rain is lost as the result of a variety of factors. Among the main factors contributing to rain loss are (a) evaporation and transpiration, (b) retention by vegetation and by topographic details of the terrain (including minor ponds), and (c) surficial infiltration and deep percolation, depending on the type of soil cover and geological characteristics of the region. The difference between total rain and losses other than those from rapid-drainage flowing-through-cover soil water is the excess rain defined here as runoff.

Runoff is evacuated relatively rapidly from the watershed via open channels and rivers that lead to the reservoir entrance (point B in the schematic representation in Figure 1), where the runoff flow Q(t) can be measured (Figure 2).

The storm total rain is translated into incremental runoff using semi-empirical transformations (Miller and Clark 1960) that include consideration of a complex index to classify the watershed according to the cover soil and the land use. This piecewise-constant effective water-input history is applied to the watershed hourly

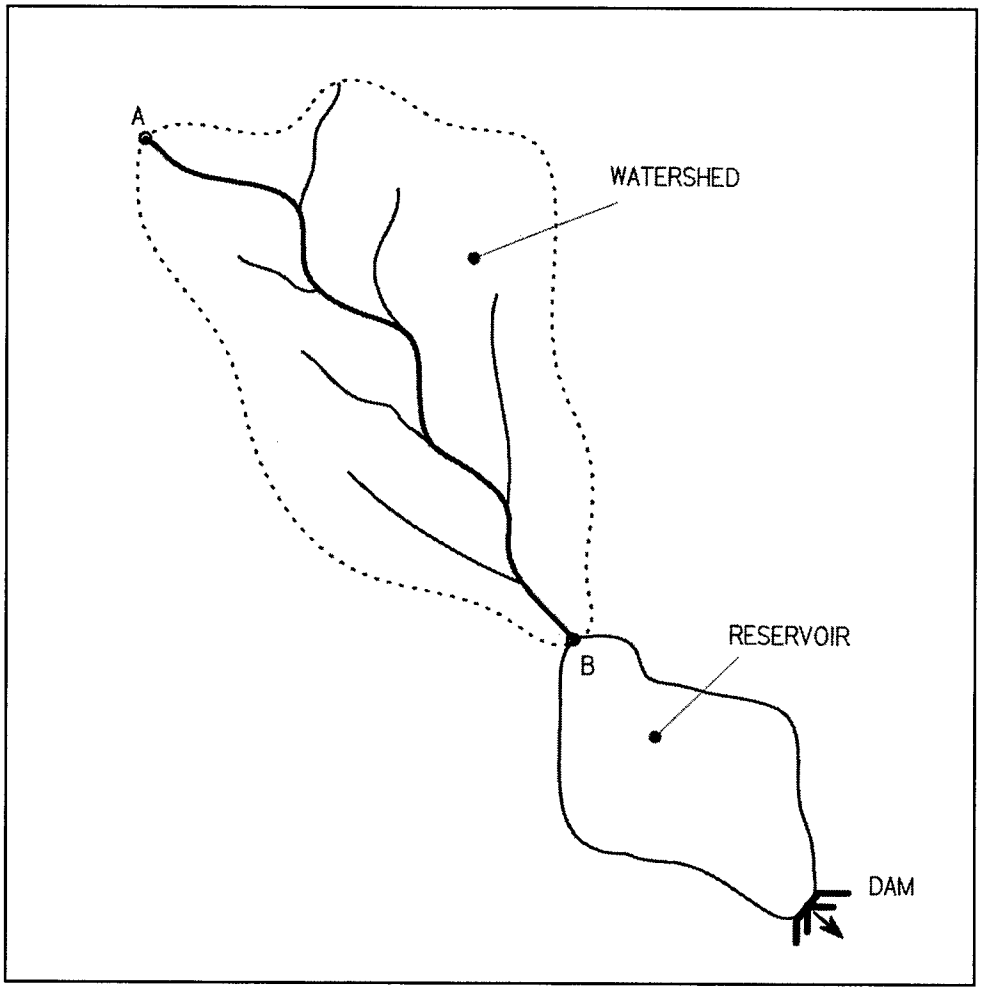

Figure 1. Schematic plan view of a watershed-reservoir-dam system

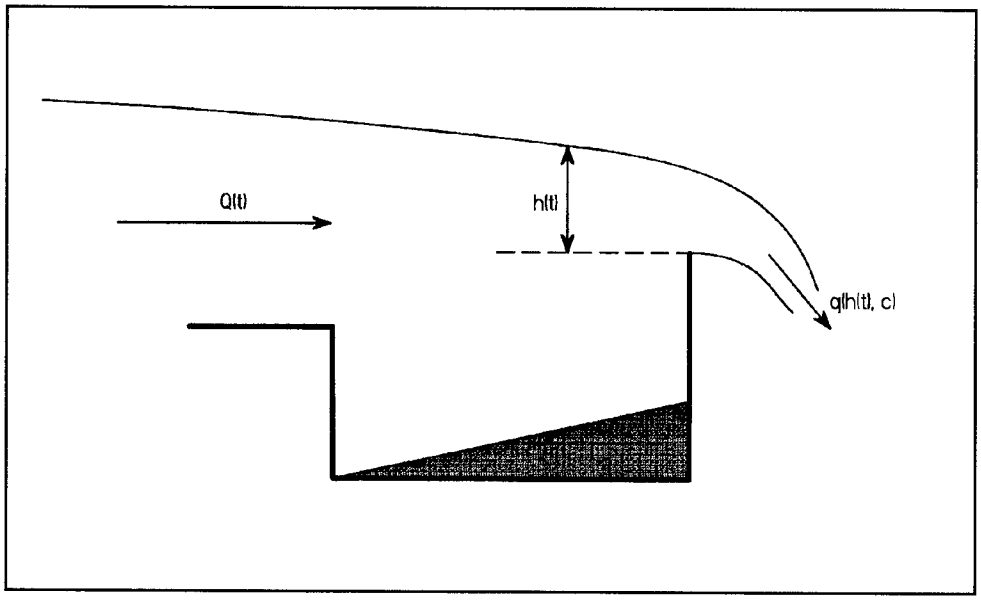

Figure 2. Longitudinal section of analytical model of a reservoir

during the first 6 hr of storm and, thereafter, in incremental time intervals of 6, 12, and 24 hr, respectively. It should be noted, however, that the order of hourly precipitation during the first 6 hr of storm cannot be predicted. Therefore, in this model the specific order of the rain steps for a given storm is subjected to aleatory permutation, whether the representation is deterministic or not.

Figure 2 shows the longitudinal section of the analytical model for the reservoir component in the system. The input flow $Q(t)$ represents the response of the watershed to the water-input event. The spillway outflow $q(h(t), c)$ at the opposite end of the reservoir (Figure 3) depends on the discharge coefficient c. This, in turn, is a function of the weir elevation z and of the reservoir elevation $h(t)$ itself, giving rise to a highly nonlinear governing differential equation for the response. The reservoir water level over the spillway crest $h(t)$ is directly related to the storm-water storage and represents the hazard on the dam structure whose safety is to be evaluated later in terms of the potential modes of failure of overtopping, overstressing, overturning, and sliding instability. For simplicity, the pool level at the beginning of the storm is considered to be that of the spillway crest, but any other convenient datum may be defined by the analyst at will.

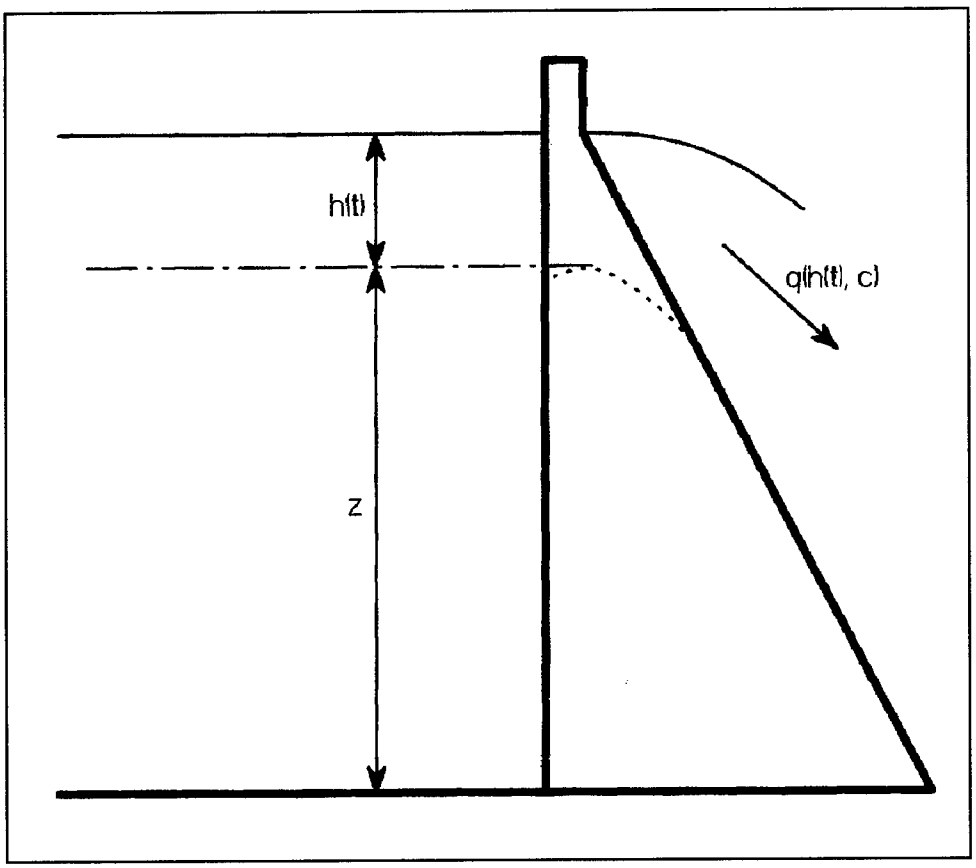

Figure 3. Transverse section of analytical model on nonoverflow dam monolith (Spillway crest is schematically represented by the dotted line)

Notice that the model differs from the real reservoir by the fact that the bottom of the reservoir may be randomly covered with sediments over time and also that our topographical surveys are imperfect, particularly in the vicinity of the boundary of the reservoir. The corresponding effects on the governing differential equation for the reservoir response are optionally included in the probabilistic version of the model by adding a Gaussian noise component to the input random process.

Convex Unitgraph

The convex model for the response of a watershed to a water-input event is based on the principle of continuity and on a postulated linear relationship between the response flow $Q(t)$ and the watershed storage $S(t)$. When the storm inflow is constant, the governing differential equation may be expressed (Dingman 1994) as:

$$\frac{dS}{dt}+\left(\frac{1}{T*}\right)\cdot S=\omega_0 \tag{1}$$

where T^* = centroidal lag between the inflow and outflow hydrographs

This is taken as a constant characteristic of the watershed. The solution to this equation under zero initial conditions is:

$$Q(t)=\frac{S(t)}{T*}=\omega_0\cdot\left(1-e^{-k*t}\right) \qquad 0\le t\le t_\omega \tag{2}$$

where $k^* = 1/T^*$

This result indicates that the output response approaches asymptotically the inflow ω_0 as far as the termination of the water-input event t_ω. At this time, the recession limb of the response starts an exponential decay toward the zero-flow value. This means that the time to concentration of the model tends to infinity, similarly to the time to concentration of a real watershed. The recession limb of the response is given by:

$$Q(t)=q_{pk}\cdot e^{-k*\cdot(t-t_\omega)} \qquad t>t_\omega \tag{3}$$

where $q_{pk} = Q(t_\omega)$ is the maximum value of the outflow

Notice that the only parameter characterizing the response is T^*, which may be estimated as:

$$T*=\frac{L_r}{U_w} \tag{4}$$

where

L_r = length of the longest reach in the drainage basin (distance between points A and B along the stream in Figure 1)

U_w = velocity of propagation of the flood wave

The convex unitgraph is defined in this investigation as the outflow response of the watershed to a constant-rate water-input event with a total volume of unit value (usually a volume of rain with 1 in. of depth and uniformly distributed over the whole drainage area). The duration of this constant-rate water-input event is the unit period, which in this model is taken as 1 hr.

Watershed Response Hydrograph

The watershed response hydrograph is obtained by superposition in time of the scaled hydrographs corresponding to the actual incremental effective rain volumes (usually expressed in inches of rain uniformly distributed over the whole watershed area). Analytically, this procedure can be generalized by considering the response to a unit-volume input rain concentrated at the origin of time. In other words, the watershed output response is, in this case, the unit-impulse response function $u(t)$, as the input rain is a Dirac delta function at the origin of time, i.e., a zero-duration unit-volume rain at $t = 0$. In this case, the governing differential equation for the watershed becomes:

$$T^* \cdot \frac{du}{dt} + u(t) = \delta(t) \tag{5}$$

with initial condition u(0) = 0. The general solution of this equation is:

$$u(t) = A \cdot e^{-k^* \cdot t} \tag{6}$$

The constant of integration A may be obtained by integrating Equation 5 over the infinitesimal time interval $(-\varepsilon,+\varepsilon)$ and taking the limit as $\varepsilon \rightarrow 0$ to get the unit-impulse response function as:

$$u(t) = k^* \cdot e^{-k^* \cdot t} \qquad t > 0 \tag{7}$$

The watershed response hydrograph to an inflow with the rate of rain $r(t)$ may be obtained by superposition in the time domain and is given by the convolution integral:

$$Q(t) = \int_{0^+}^{t} r(t-\tau) \cdot u(\tau) \cdot d\tau \qquad t > 0 \tag{8}$$

In fact, the response to $r(t) = \omega_0$ = constant may also be obtained as the expressions in Equations 2 and 3 by direct evaluation of Equation 8.

Figure 4 shows a family of these responses for a storm with magnitude ω_0 = 100 Ksec-ft acting during 4 hr. The parameter T^* for the family of curves varies from a value T^* = 25 hr (a slow-evacuation watershed) to a value T^* = 2.5 hr (a rapid-evacuation watershed). The 'slow' watersheds have smaller peak values of outflow and larger residual flows at the end of the period under consideration

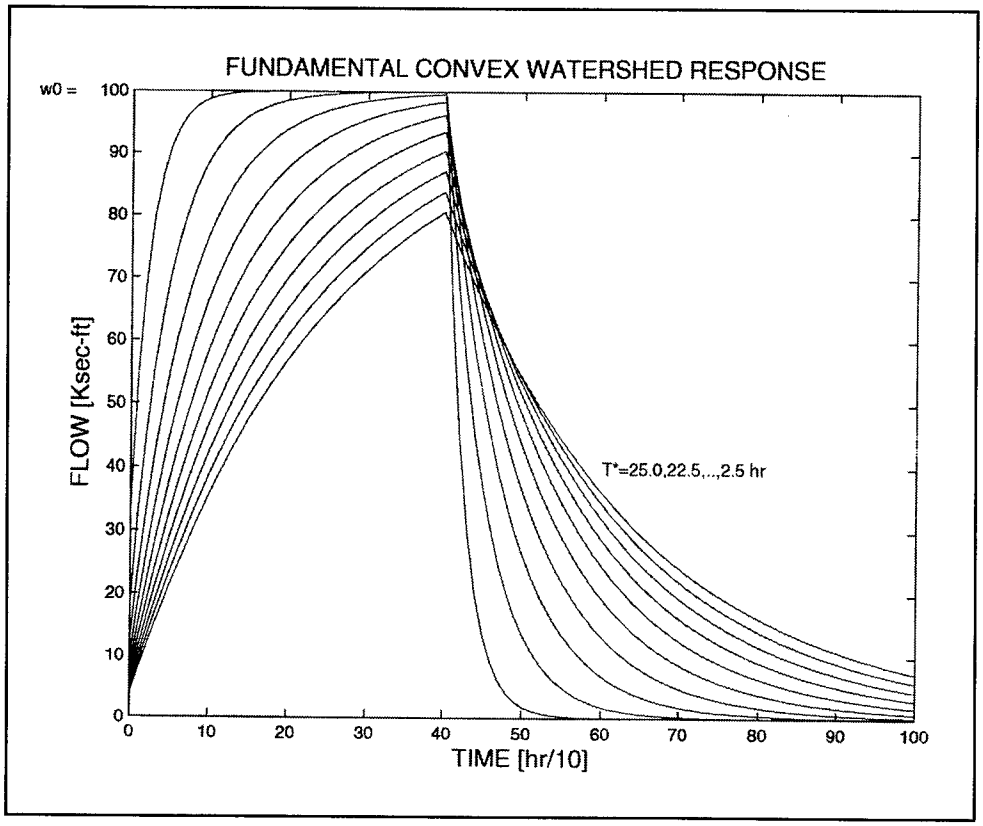

Figure 4. Family of convex-watershed responses to a uniform runoff flow w_0 acting during a finite time interval (4 hr). Curves in the set are characterized by the centroidal lag time T*

(10 hr). On the other hand, the 'rapid' watersheds often get almost to the asymptotic value ω_0 within the storm duration and rapidly decay toward zero residual flow upon storm termination.

The procedure described up to this point to construct the inflow design flood hydrograph into the reservoir (i.e., the watershed outflow hydrograph) is shown in the flow diagram in Figure 5. This schematic structure is followed in both the deterministic and the probabilistic versions of the model being constructed. Again, the probabilistic model concentrates on the effects of a random water-input event magnitude and of a random watershed centroidal lag T^*.

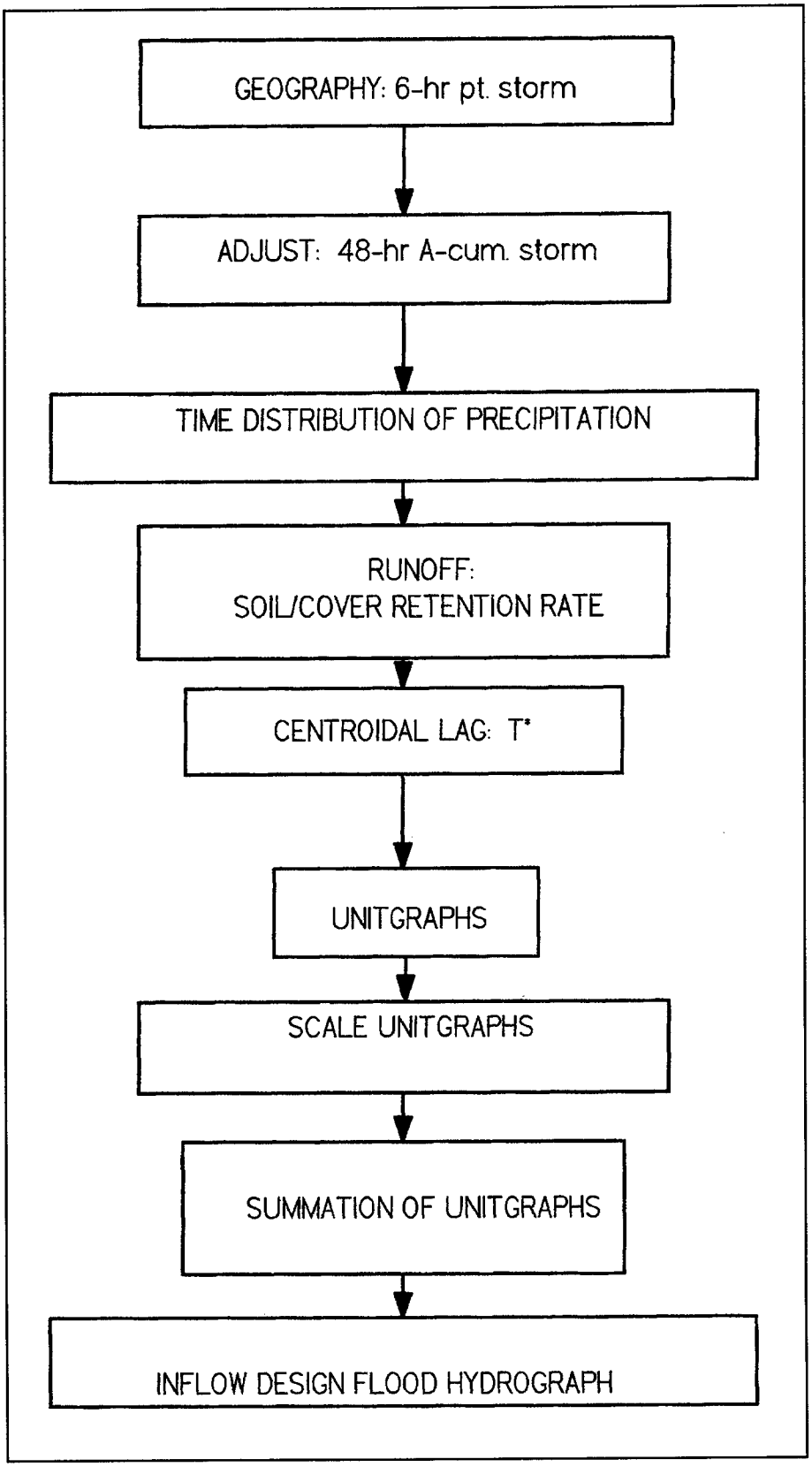

Figure 5. Procedure to construct an inflow-flood hydrograph for a typical reservoir

3 Deterministic Studies

An examination of the physical quantities entering the deterministic formulation for the response of the watershed-reservoir-dam system to a water-input event and its sensitivity to variations in those quantities proves to be insightful in revealing the fundamental nature of the relations involved.

Watershed Routing

In this model, the response of the watershed-reservoir-dam system is followed for a time interval of 60 hr after the beginning of the storm, which is assumed to last 48 hr. The subscript I = 1,2,...,6 refers to the first six 1-hr intervals; I = 7,8,9 refers to the time intervals following the first 6 hr of storm duration with time lengths of 6, 12, and 24 hr, respectively; and i = 10 refers to the last 12 hr of rain-free history of response.

The procedure to determine the incremental runoff during each of these intervals follows the standard and well accepted recommendations in practice (Miller and Clark 1960; USBR 1976, 1977). According to the geographical location and extension of the watershed, the 6-hr 'point' PMP is distributed in time and expressed as the accumulative rain fall in the actual-size watershed at the end of each of the intervals described above (r_i, i = 6,..,9). This distribution may be expressed as:

$$r_{i+5} = a_i \cdot \rho \qquad i = 1,\ldots,4 \tag{9}$$

where

ρ = 6-hr 'point' PMP

a_i = empirical coefficient

Likewise, the accumulative rainfall at the end of each of the first six 1-hr intervals may be expressed as:

$$r_i = b_i \cdot r_6 \qquad i = 1,\ldots,6 \tag{10}$$

where

r_6 = the accumulative total rain at the end of 6 hr of storm, as provided by Equation 9

b_i = empirical coefficient

Therefore, the incremental total rain corresponding to each of the first 1-hr intervals is given by:

$$\begin{aligned} \Delta r_1 &= r_1 \\ \Delta r_i &= r_i - r_{i-1} \qquad i = 2,\ldots,6 \end{aligned} \tag{11}$$

Again, the order of these first six 1-hr incremental contributions to the total precipitation cannot be predicted, and they are given an aleatory permutation, after which the accumulative total rain is recalculated according to:

$$\begin{aligned} r_1 &= \Delta r_1 \\ r_i &= r_{i-1} + \Delta r_i \qquad i = 2,\ldots,9 \end{aligned} \tag{12}$$

Next, the accumulative and incremental effective precipitations (direct runoff) are calculated. These calculations require the estimation of the local hydrologic soil-cover complex number (S), according to the soil-series classification and the combined land use at the site (USBR 1976, 1977), modified according to the antecedent conditions. The U.S. Soil Conservation Service (Miller and Clark 1960) recommends the use of the following fit to estimate runoff (based on numerous statistical studies and assuming the initial abstraction as $I_a = 0.2 \cdot S$):

$$p_i = \frac{(r_i - 0.2 \cdot S)^2}{r_i - 0.8 \cdot S} \qquad i = 1,\ldots,9 \tag{13}$$

where p_i = accumulative runoff at the end of the i-th time interval, and

$$\begin{aligned} \Delta p_1 &= p_1 \\ \Delta p_i &= p_i - p_{i-1} \qquad i = 2,\ldots,9 \end{aligned} \tag{14}$$

where Δp_i = incremental runoff corresponding to the i-th time interval

There is a physical lower bound for the hourly loss during each interval (Miller and Clark1960). In this model, the hourly loss is not allowed to be less than 0.05 in. Upon insertion of this minimum value, the incremental runoff is recalculated for each interval as:

$$\Delta p_i^* = \Delta r_i - \Delta L_i \qquad i = 1,\ldots,9 \tag{15}$$

and

$$\begin{aligned} p_1^* &= \Delta p_1^* \\ p_i^* &= \Delta p_i^* + p_{i-1} \qquad i = 2,\ldots,9 \end{aligned} \tag{16}$$

where ΔL_i is the total loss corresponding to the i-th interval, and symbols with an attached asterisk correspond to the recalculated quantities.

The watershed routing is completed using the convolution integral of Equation 8 reformulated for computational analysis. When the input effective precipitation is represented by a piecewise constant function, Equation 8 gives

$$Q(t)=\sum_{i=1}^{9} q_{pk,i}\cdot e^{-k^*\cdot(t-t_i)} \qquad t>t_\omega$$

i.e.,

$$Q(t)=\sum_{i=1}^{9}(Recess)_i \tag{17}$$

where

$(Recess)_i$ = contribution of the recession limb of the response to the i-th increment of direct runoff when acting alone during the time interval ending at t_i

$q_{pk,i}$ = corresponding maximum response, as in Equation 3, and

$$Q(t)=\sum_{i=1}^{j}(Recess)_i + p_{j+1}\cdot\left[1-e^{-k^*\cdot(t-t_j)}\right] \qquad t_{j<t\le t_\omega}\ \ j\ge 0 \tag{18}$$

when the response is evaluated within the $(j+1)$-th interval and $t_0 = 0$

Reservoir Routing

The outflow from the routing of rain fall through the watershed represents the inflow for the reservoir component. Based on the principle of continuity, the governing differential equation for the reservoir routing in terms of the pool at the upstream face of the dam, $h(t)$, is given by (Jiang 1998):

$$\frac{dh}{dt}=\frac{Q(t)-q\left[h(t),c\right]}{G\left[h(t)\right]} \tag{19}$$

where

$Q(t)$ = inflow from the watershed given by Equations 17 and 18

$q(h(t),c)$ = outflow through the spillway weir

c = corresponding discharge coefficient

$G(h)$ = gradient of variation of the reservoir storage as a function of the reservoir pool

Notice that other outlet works may be included in $q(h(t),c)$, if present. In this model, for simplicity, only a rectangular spillway weir is considered. The outflow

through a rectangular weir may be estimated by (Street, Watters, and Vennard 1996):

$$q\left[h(t),c\right]=\frac{2}{3}\cdot b\cdot c\cdot\sqrt{2g}\cdot h(t)^{3/2} \tag{20}$$

where

b = weir length

c = discharge coefficient

g = acceleration of gravity

Von Mises has developed a simple semiempirical expression for the coefficient of discharge as (Olson 1961):

$$c=0.611+0.075\cdot\frac{h(t)}{z} \tag{21}$$

where z is the height of the spillway crest over the reservoir bottom (Figure 3).

The reservoir storage may be regressed empirically as a quadratic function of the reservoir pool (Jiang 1998), leading to a linear fit for the corresponding gradient, so that it may be expressed as:

$$G(h)=a+\beta\cdot h \tag{22}$$

where α, β are empirical coefficients for the reservoir being considered.

Inserting Equations 17, 18, 20, 21, and 22 into Equation 19 leads to a nonlinear ordinary differential equation for h(t) that can be solved numerically (The MathWorks 2000).

Computational Analysis

The watershed centroidal lag is estimated in the computational implementation of the model using the empirical equation inferred by the California Highways and Public Works (Miller and Clark 1960):

$$T^{*}=\left(\frac{11.9\cdot L^{3}}{H}\right)^{0.385} \tag{23}$$

where

L = length of the longest watercourse in miles (i.e., the distance between points A and B along the stream in Figure 1)

H = elevation difference (between the same points A and B in Figure 1) in feet

T^* = obtained in hours

Figure 6 shows a Graphical User Interface (GUI) implemented in Matlab 6.0 (The MathWorks 2000) with the data for a sample watershed-reservoir-dam system in zone 7 east of the 105° meridian. The program builds the hydrographs for the inflow design flood into the reservoir and for the pool, for the design storm (PMP), and provides the analyst with instant feedback. The command Plot Hydrographs on the lower right corner of the GUI invokes the callback routines that execute the convex routing algorithm with immediate results useful for either the design of new hydraulic structures or the evaluation of existing facilities against overtopping.

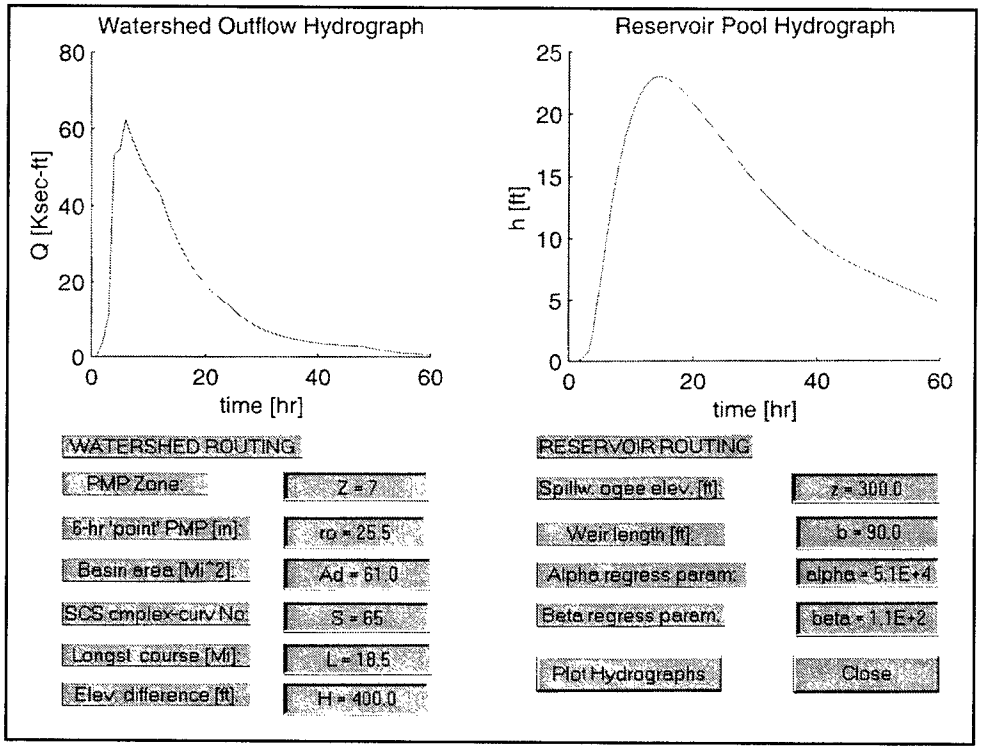

Figure 6. GUI designed for ready estimation of deterministic design hydrographs

Surface Hydrographs

The watershed outflow hydrograph and the associated reservoir pool hydrograph are then generated for a drainage basin with a continuously varying centroidal lag. Figures 7 and 8 show the resulting surface hydrographs for a rather severe design storm with PMP = 30 in. Notice the pronounced peak of the hydrographs (i.e., of the trace of the corresponding surface on the plane T^* = constant) for watersheds with rapid evacuation characteristics (relatively short T^*) and the small residual quantity at the end of the response history. Watersheds with slow evacuation characteristics (relatively long T*) tend to remain flat in time, and therefore show larger residual quantities at the end of the response

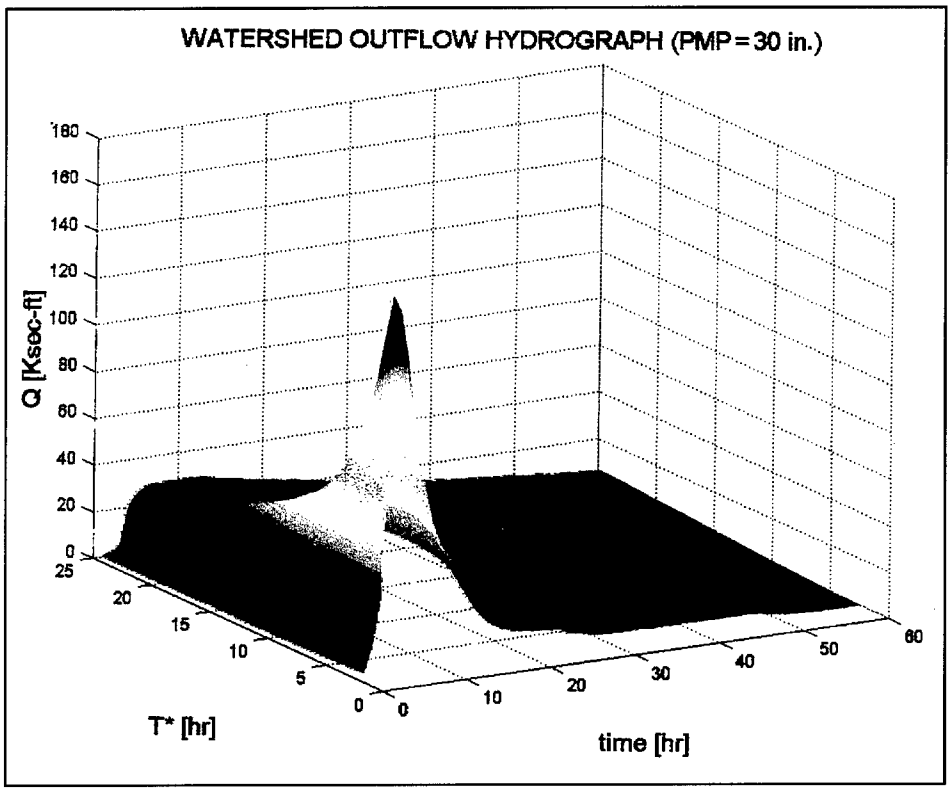

Figure 7. Three-dimensional representation of a typical watershed outflow hydrograph surface (Deterministic PMP = 30 in.)

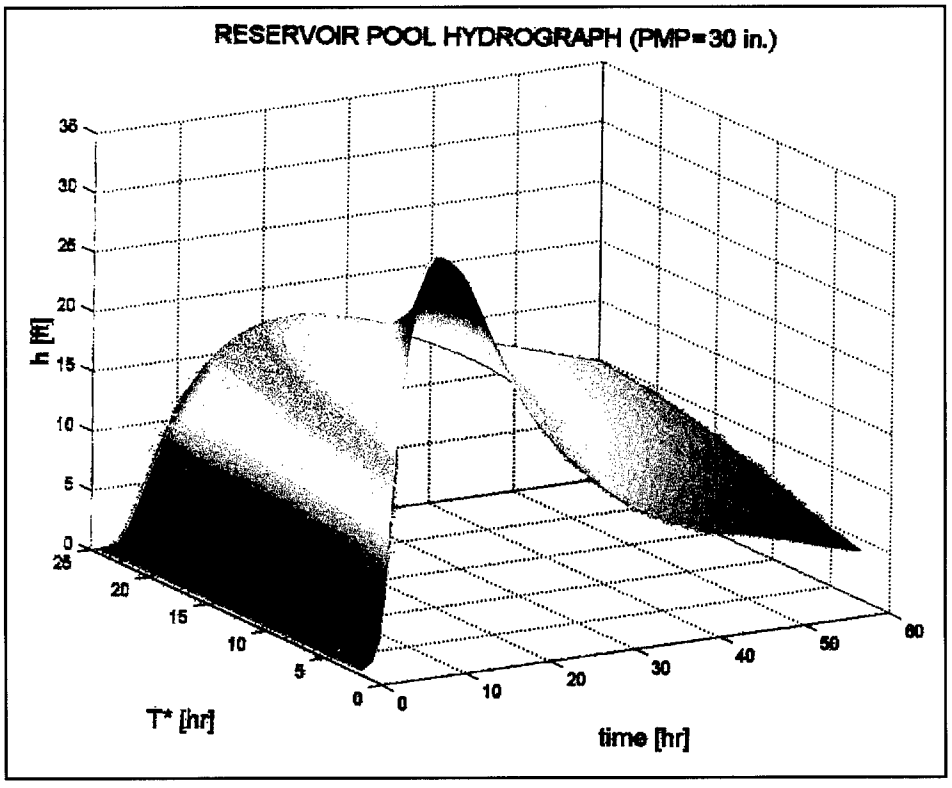

Figure 8. Three-dimensional representation of a typical reservoir pool hydrograph surface (Deterministic PMP = 30 in.)

history. Figures 9, 10, 11, and 12 show these hydrographs for selected PMP specific values of 30 and 20 in., respectively. The trends in the family of curves remain the same with the smaller magnitudes of response associated with the smaller design storms.

Similarly, hydrographs for watershed outflow and for the corresponding reservoir pool are built for a fixed watershed, with a varying magnitude of the water-input event (PMP = 15 to 35 in., @5 in.). Figures 13 and 14, and 15 and 16 show two sets of hydrograph families for a rapid-evacuation watershed (T* = 5 hr) and for a slow-evacuation watershed (T* = 15 hr). Both sets tend to support the basic assumption under the standard unitgraph superposition principle applied in practice that the response hydrographs essentially retain their shapes with the ordinates amplified in proportion to the magnitude of the water-input event (PMP).

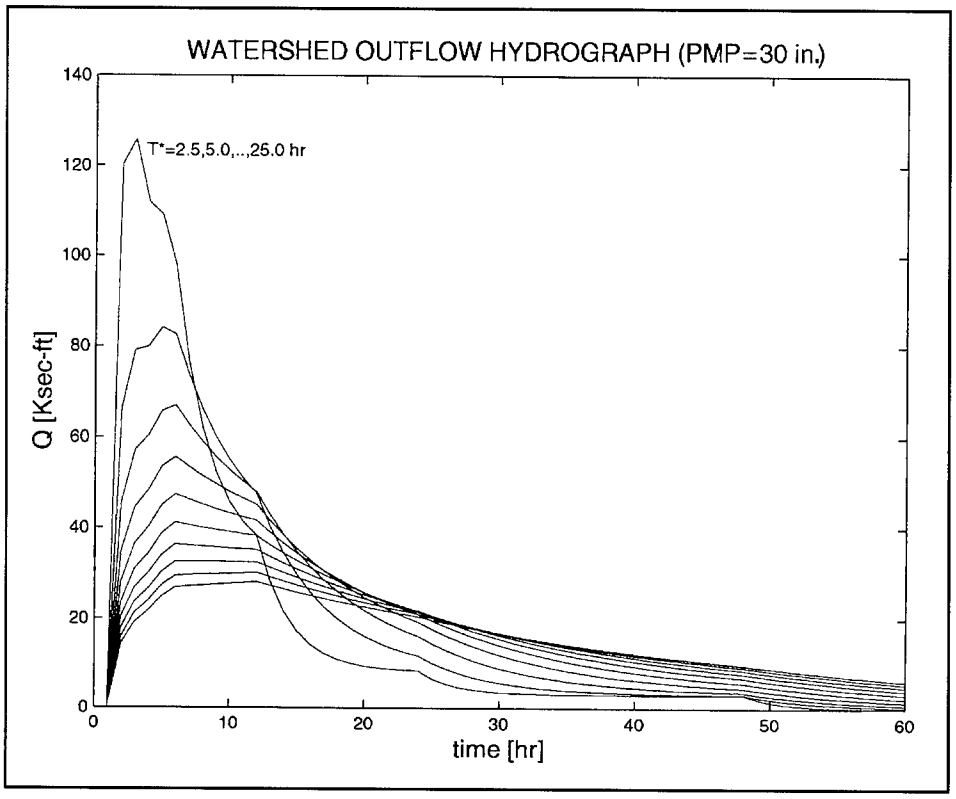

Figure 9. Family of traces of the hydrograph surface shown in Figure 7 with a set of planes T^* = constant

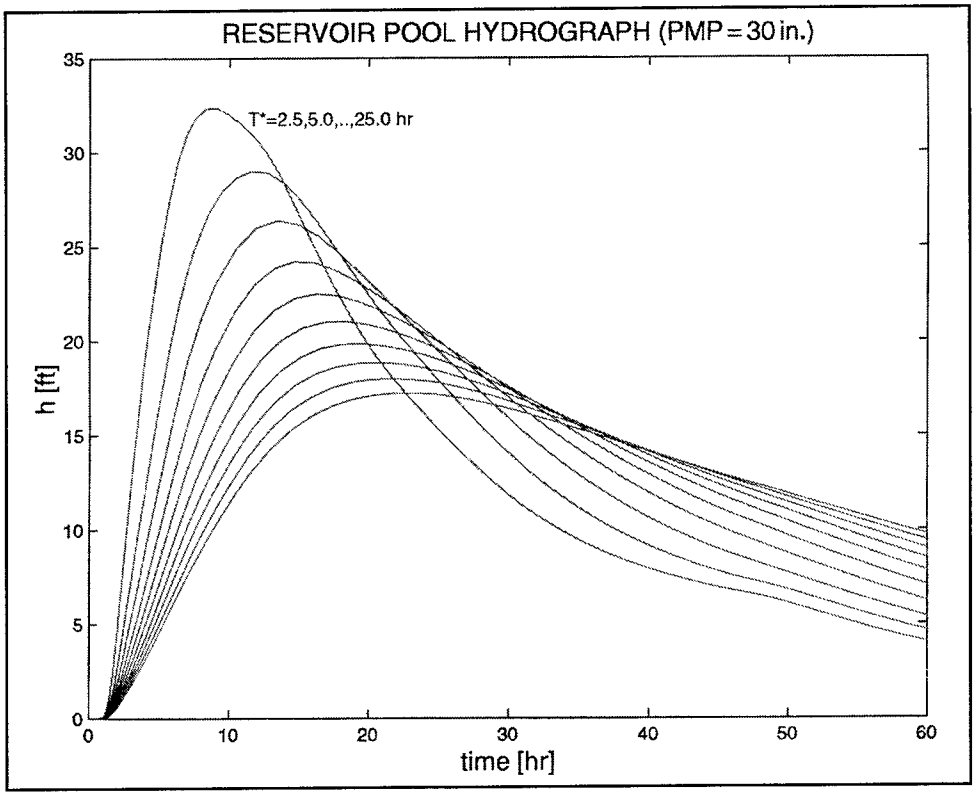

Figure 10. Family of traces of the hydrograph surface shown in Figure 8 with a set of planes T^* = constant

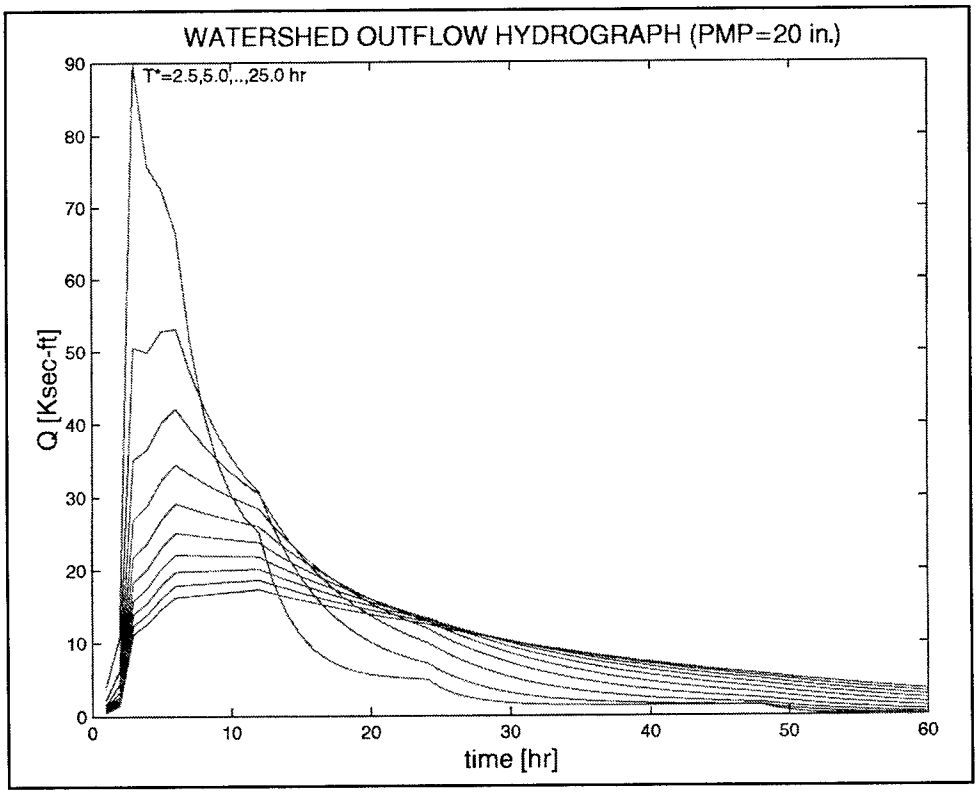

Figure 11. Family of traces of a watershed-outflow hydrograph surface built for a deterministic PMP = 20 in. with a set of planes T^* = constant

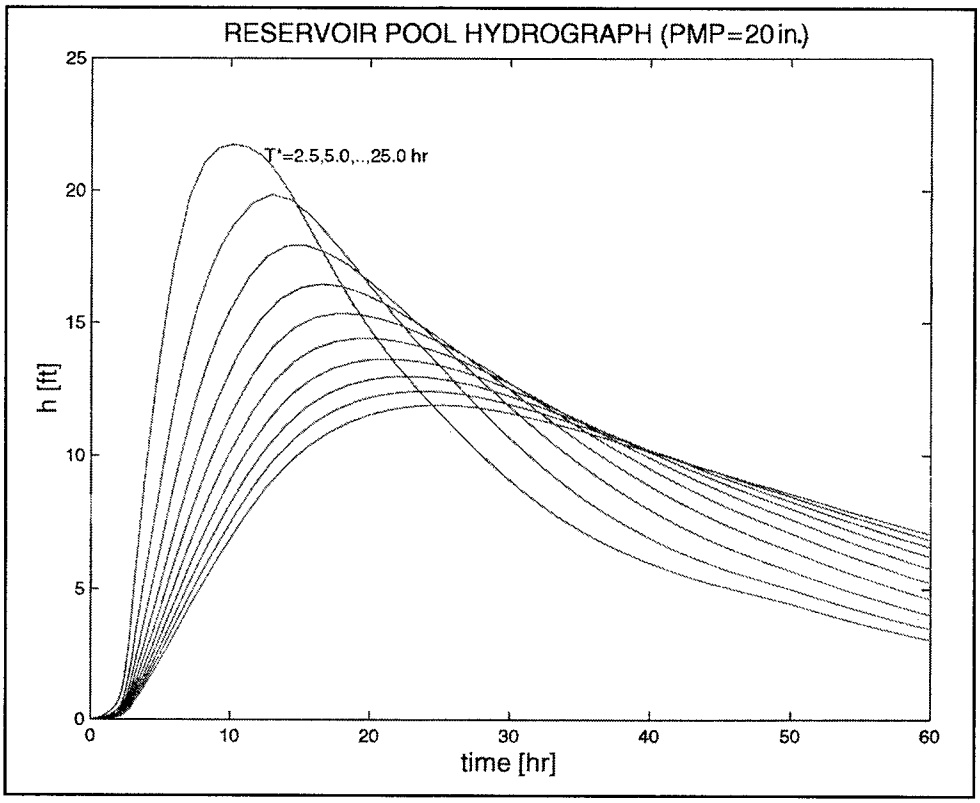

Figure 12. Family of traces of a reservoir-pool hydrograph surface built for a deterministic PMP = 20 in. with a set of planes T^* = constant

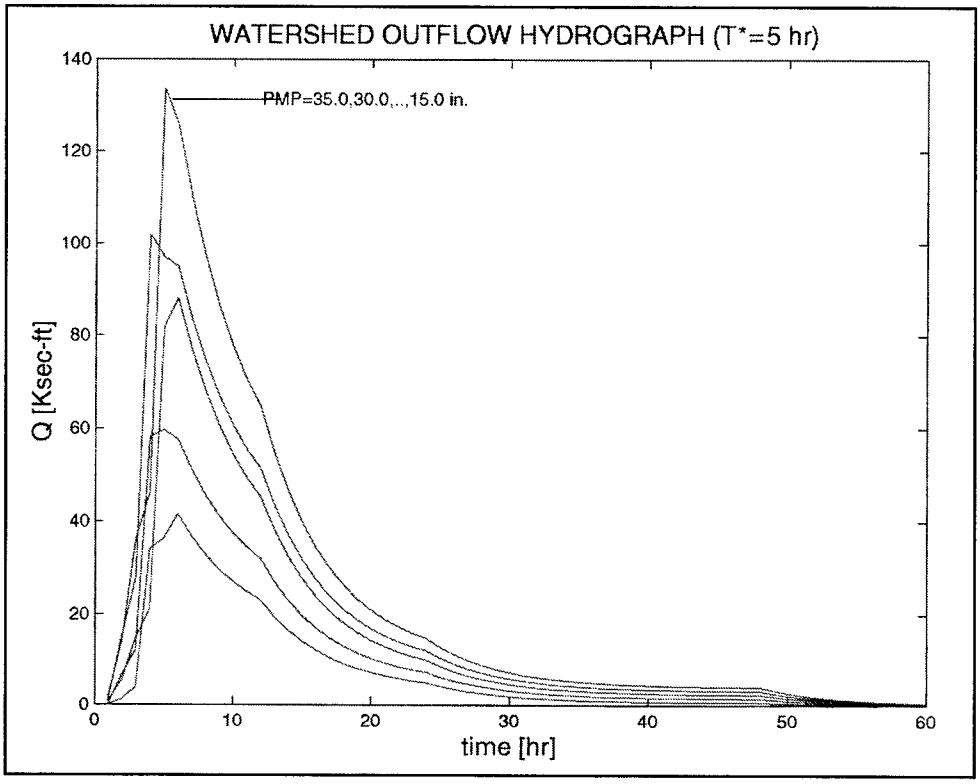

Figure 13. Family of reservoir inflow-flood hydrographs built for a deterministic watershed with a relatively short centroidal lag time (T^* = 5 hr) for several values of the water-input event PMP

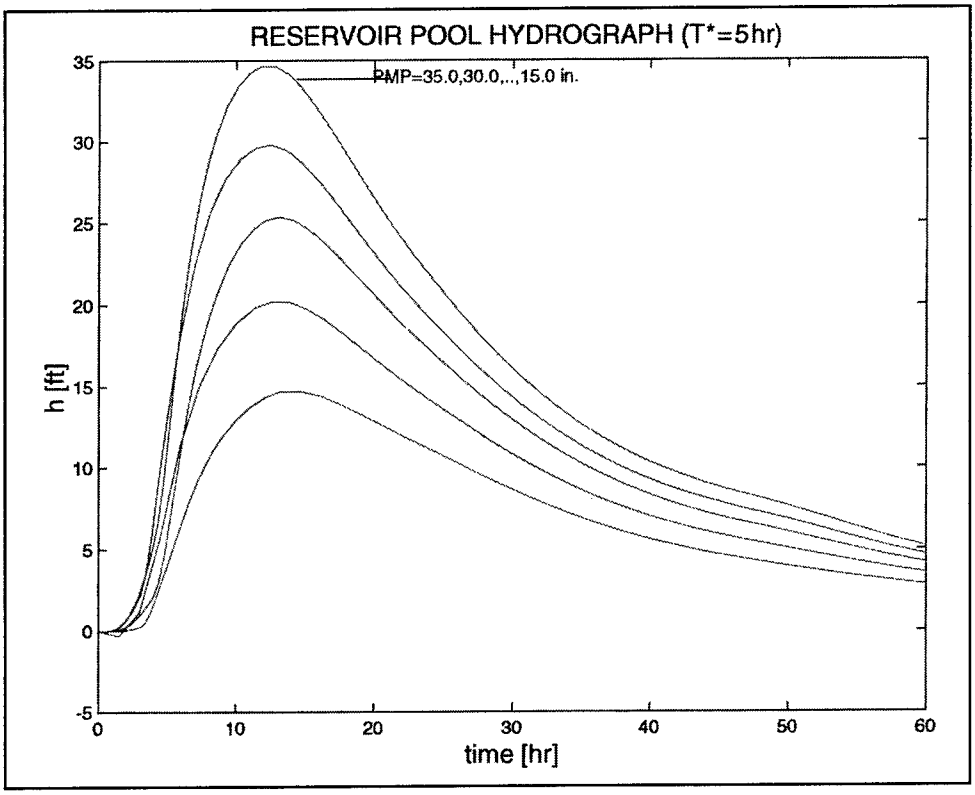

Figure 14. Family of reservoir-pool hydrographs built for a deterministic watershed with a relatively short centroidal lag time (T^* = 5 hr) for several values of the water-input event PMP

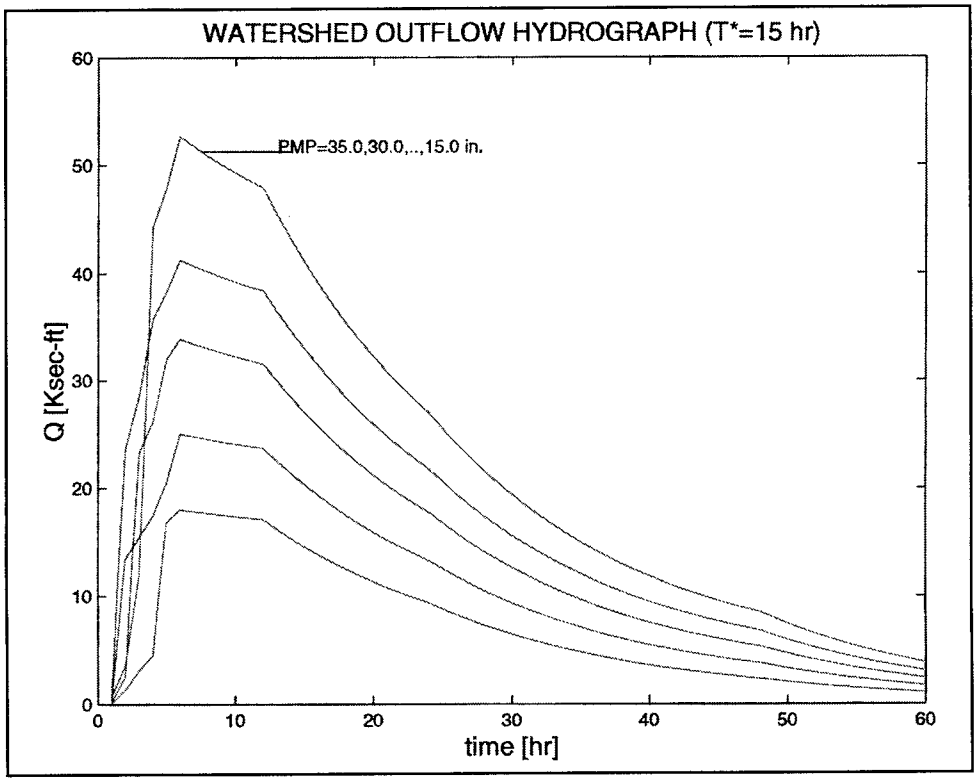

Figure 15. Family of reservoir inflow-flood hydrographs built for a deterministic watershed with a relatively long centroidal lag time (T^* = 15 hr) for several values of the water-input event PMP

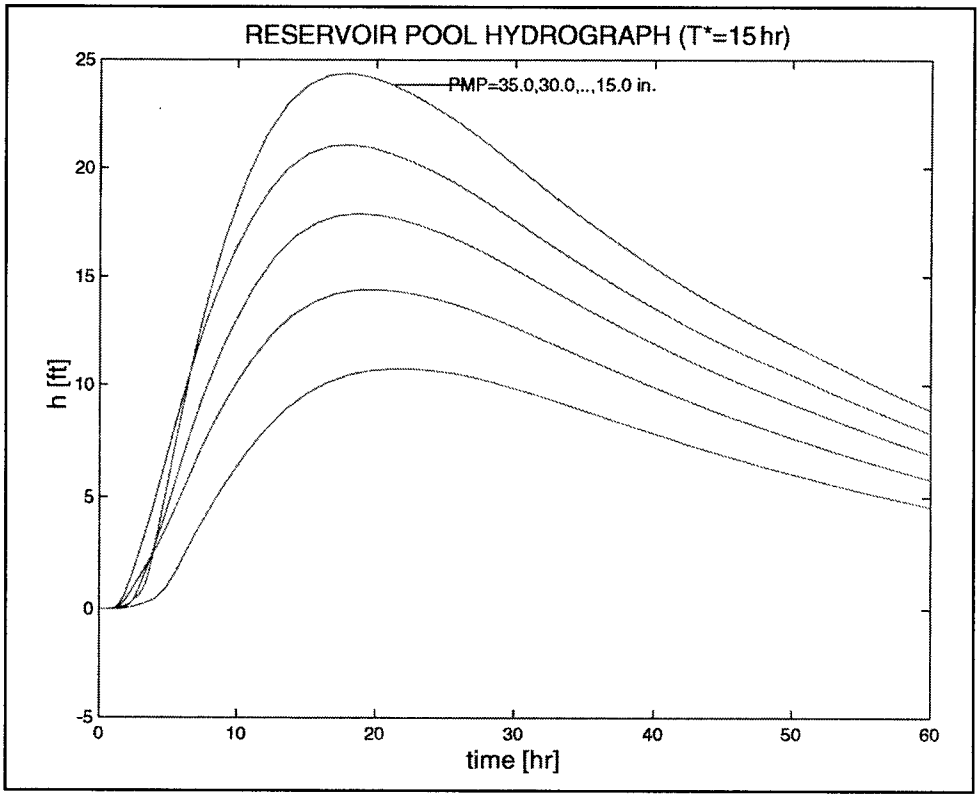

Figure 16. Family of reservoir-pool hydrographs built for a deterministic watershed with a relatively long centroidal lag time (T^* = 15 hr) for several values of the water-input event PMP

Response Spectra

The peak values of response in terms of the watershed outflow and the reservoir pool may be recorded for a continuous variation of the centroidal lag and with the magnitude of the water-input event (PMP) as a parameter. The resulting family of curves constitute the response spectra for the response quantity under consideration. Figures 17 and 18 show the response spectra for the watershed outflow $Q(t)$ and for the reservoir pool $h(t)$.

The set of response spectra for the watershed outflow is very sensitive to the particular order of the resulting aleatory permutation of the hourly storm precipitation values during the first 6 hr of the water-input event. More unfavorable system responses are obtained when the largest incremental rain value occurs during the sixth storm hour than the responses for those storms in which the largest incremental rain value occurs during the first hour. This sensitivity becomes apparent for the rapid-evacuation watersheds (those with relatively short T^*), as evidenced by the nonsmooth gradient of Q,max with respect to the storm magnitude (PMP) in Figure 17.

By contrast, the set of spectra for the reservoir pool exhibit relatively smooth transitions when the storm magnitude (PMP) is varied. There are two fundamental reasons for this behavior: (a) the peak response of $h(t)$ for a given hydrograph

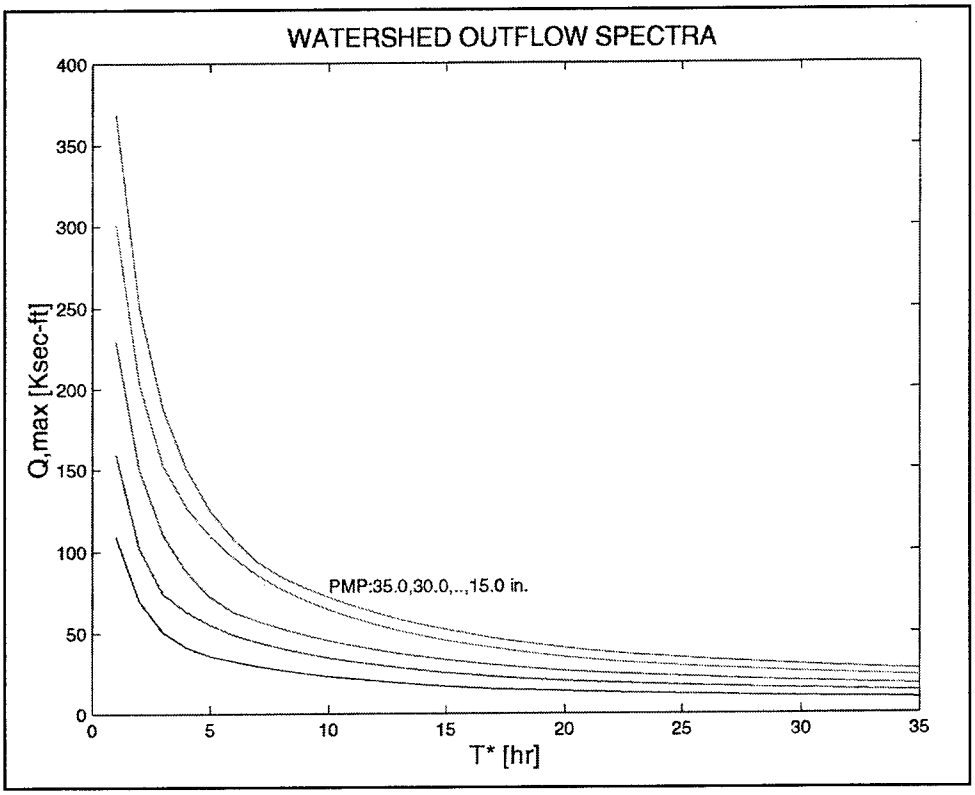

Figure 17. Family of watershed outflow spectra for several values of the water-input event PMP

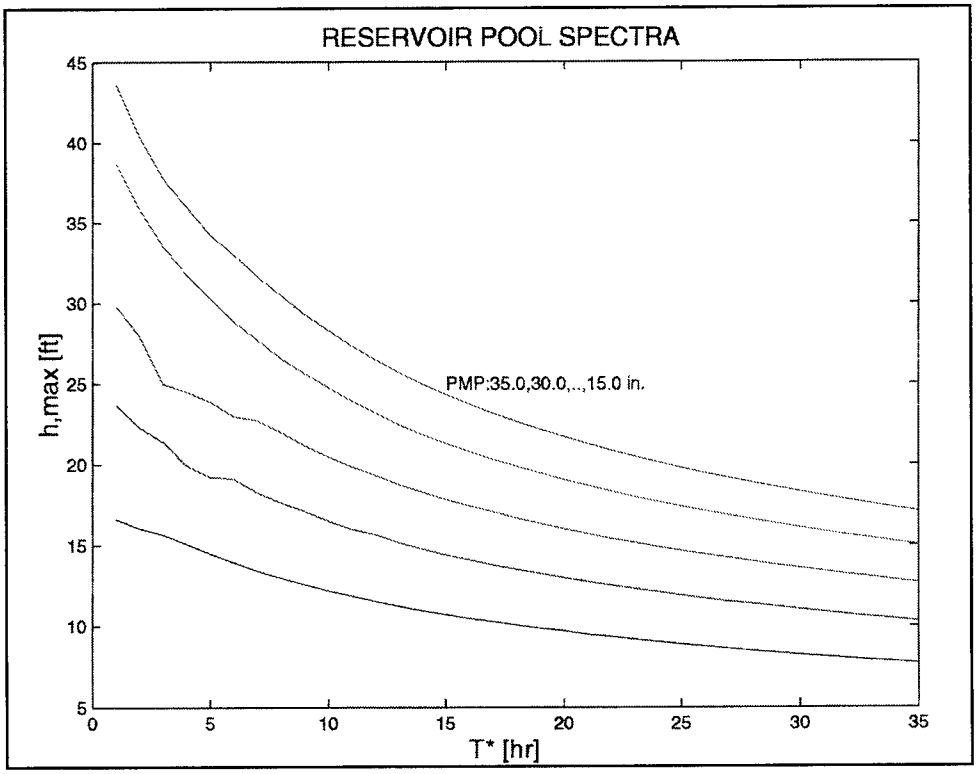

Figure 18. Family of reservoir pool spectra for several values of the water-input event PMP

systematically shows a delay with respect to the peak of $Q(t)$ (Figure 6), occurring at some time-distance of the particular hourly incremental rain lumps during the first 6 hr of storm, and (b) the peak response of $h(t)$ occurs after a second filter in the system has acted on the water input to the watershed. The reservoir pool spectra in Figure 18 can be closely approximated by the following useful mathematical expression:

$$h_{\max} = h_2(T^*) + \frac{\left[h_1(T^*) - h_2(T^*)\right]}{20} \cdot (PMP - 15) \qquad PMP \geq 15 \qquad (24)$$

where

$$h_1(T^*) = 47.15 - 8.416 \cdot \ln(T^*)$$

$$h_2(T^*) = 16.82 - 0.5192 \cdot T^* + 0.007423(T^*)^2$$

and the PMP is given in inches of rain.

Residual Response

Similarly, the residual values of response in terms of the watershed outflow and the reservoir pool at the end of the observed history may be recorded and represented graphically, as in Figures 19 and 20, respectively. Now the recorded values take place at a far time-distance of the local rain distribution during the first 6 hr of storm, and the resulting curves exhibit smooth gradients with the magnitude of the water-input event (PMP). The watershed residual outflow in Figure 19 can be closely approximated by the following mathematical expression:

$$Q_r = Q_{r2}(T^*) + \frac{\left[Q_{r1}(T^*) - Q_{r2}(T^*)\right]}{20} \cdot (PMP - 15) \qquad PMP \geq 15 \qquad (25)$$

where

$$Q_{r1}(T^*) = -0.6571 + 0.1253 \cdot T^* + 0.01648(T^*)^2 - 0.0003444 \cdot (T^*)^3$$

$$Q_{r2}(T^*) = -0.06143 - 0.01471 \cdot T^* + 0.008029(T^*)^2 - 0.0001489(T^*)^3$$

and the PMP is given in inches of rain.

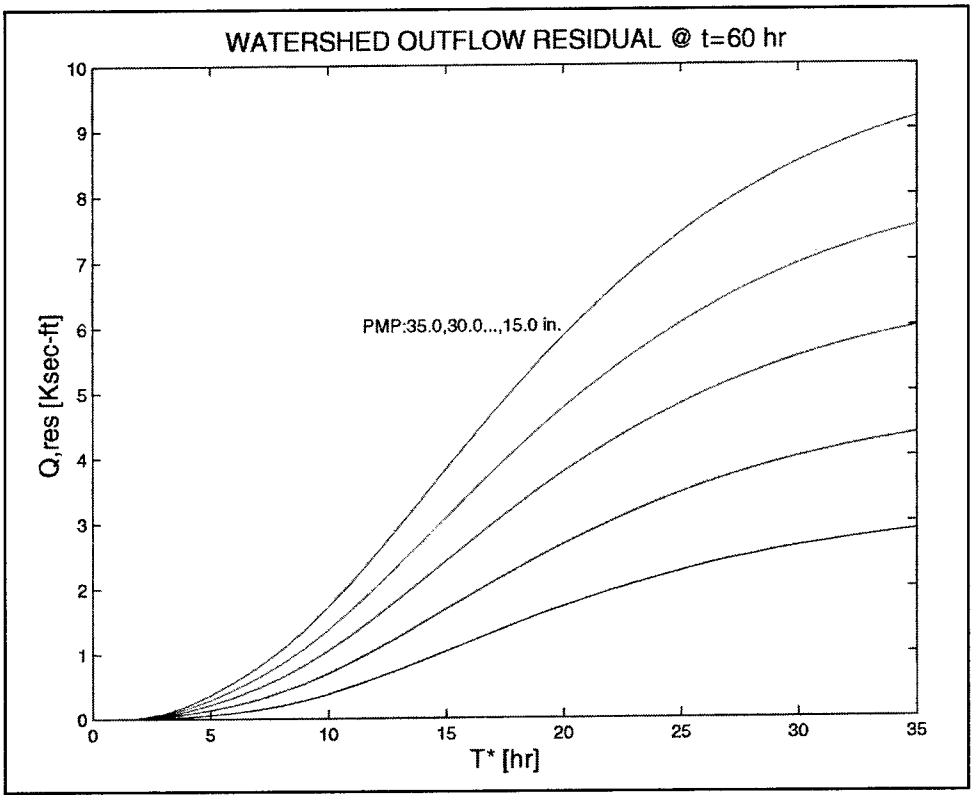

Figure 19. Family of residual watershed outflows, at the end of the history being considered (t = 60 hr), for several values of the water-input event PMP

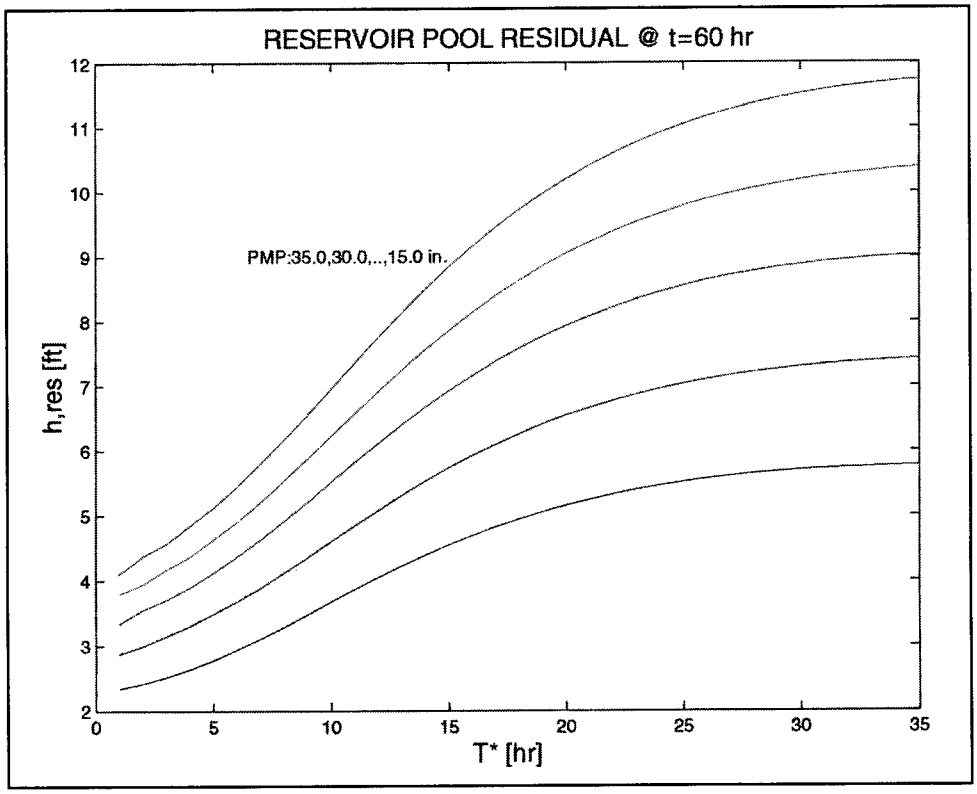

Figure 20. Family of residual reservoir pools, at the end of the history being considered (t = 60 hr), for several values of the water-input event PMP

Likewise, the reservoir residual pool in Figure 20 can be closely approximated by the following mathematical expression:

$$h_r = h_{r2}(T^*) + \frac{\left[h_{r1}(T^*) - h_{r2}(T^*)\right]}{20} \cdot (PMP - 15) \qquad PMP \geq 15 \qquad (26)$$

where

$$h_{r1}(T^*) = 3.481 + 0.3569 \cdot T^* + 0.001561(T^*)^2 - 0.0001452 \cdot (T^*)^3$$

and

$$h_{r2}(T^*) = 1.921 + 0.2061 \cdot T^* - 0.001773(T^*)^2 - (2.877E-5) \cdot (T^*)^3$$

4 Probabilistic Studies

Instantaneous Response Distributions

Next, two fundamental variables into the routing of the water-input event through the watershed-reservoir-dam system, namely the storm magnitude and the watershed centroidal lag, are assumed to be random. The 6-hr 'point' storm magnitude is modeled with the extreme-value distribution type I, of the largest values (Gumbel distribution), with mean value given by the deterministic assessment of the 6-hr 'point' PMP (Miller and Clark 1960; USBR 1976, 1977) and with a coefficient of variation estimated as 0.1. The watershed centroidal lag is assumed as log-normally distributed, with mean value given by the deterministic assessment and with a coefficient of variation estimated as 0.3. Our objective in this investigation is to identify the instantaneous distribution of the response hydrograph for the reservoir pool, $h(t)$, since this represents the effective hazard on the dam (de Béjar 1999). Sampling is conducted on the basis of Montecarlo simulations (Benjamin and Cornell 1970).

The best distribution is judged to be the log-normal distribution, fitting the data well, while being sufficiently simple for engineering applications. Figure 21 shows the quantile-quantile plot for the random variable natural logarithm of the reservoir pool at time = 24 hr, i.e., ln[h(24)], resulting from 10,000 simulated realizations of the routing of a random storm through a random watershed, with all other parameters in the deterministic system described in Figure 6. The approximate alignment with a straight line is indicative of the goodness-of-fit for engineering applications of the underlying log-normal assumption for the distribution of h(24). Figure 22 shows the nonparametric probability density function corresponding to the 10,000 simulations. Likewise, Figures 23 and 24 show the corresponding results of the 10,000 simulations for h(12). Again, the log-normal distribution is considered satisfactory for most of the data, except possibly at the tails of the distribution, where the major deviations from the model occur, as expected.

Finally, the peak values of $h(t)$ resulting from the 10,000 simulations are also processed, and again the log-normal distribution is selected as the most convenient for engineering applications. Figure 25 shows a box plot for the random variable ln[h,max] on the basis of 1,000 simulations. Only six deviant points are identified at the upper end of the presumed log-normal distribution, and only one deviant point at the lower end of the distribution. In fact, Figure 26 shows the

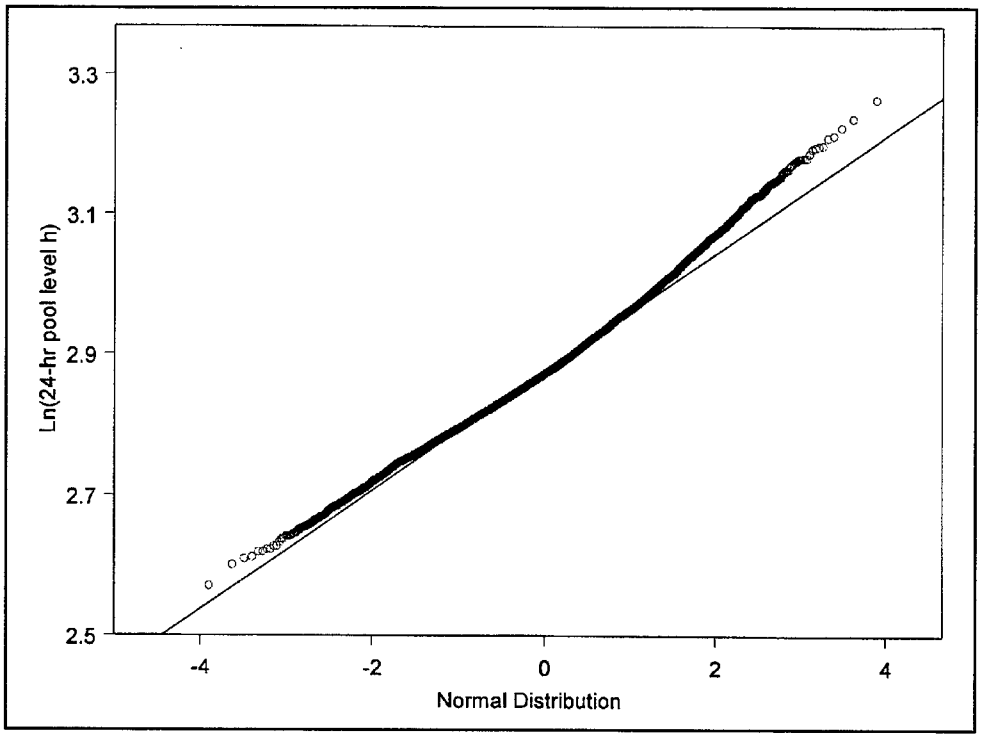

Figure 21. Quantile-quantile plot for $\log_e$ [h(24)] based on 10,000 simulations

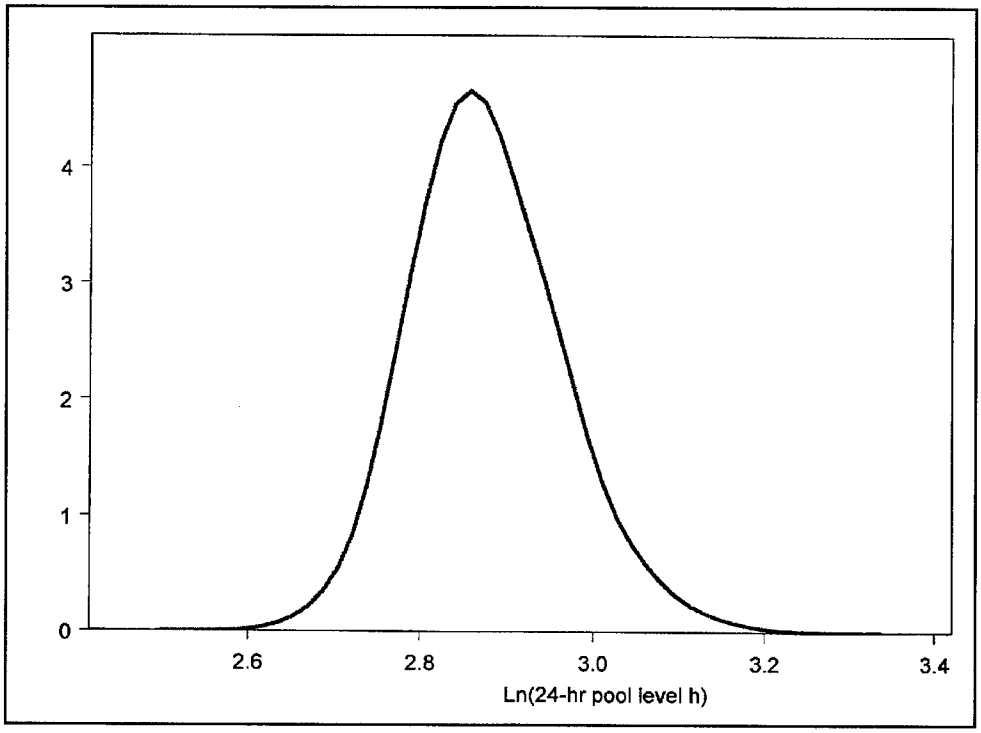

Figure 22. Nonparametric probability density for $\log_e$ [h(24)] based on 10,000 simulations

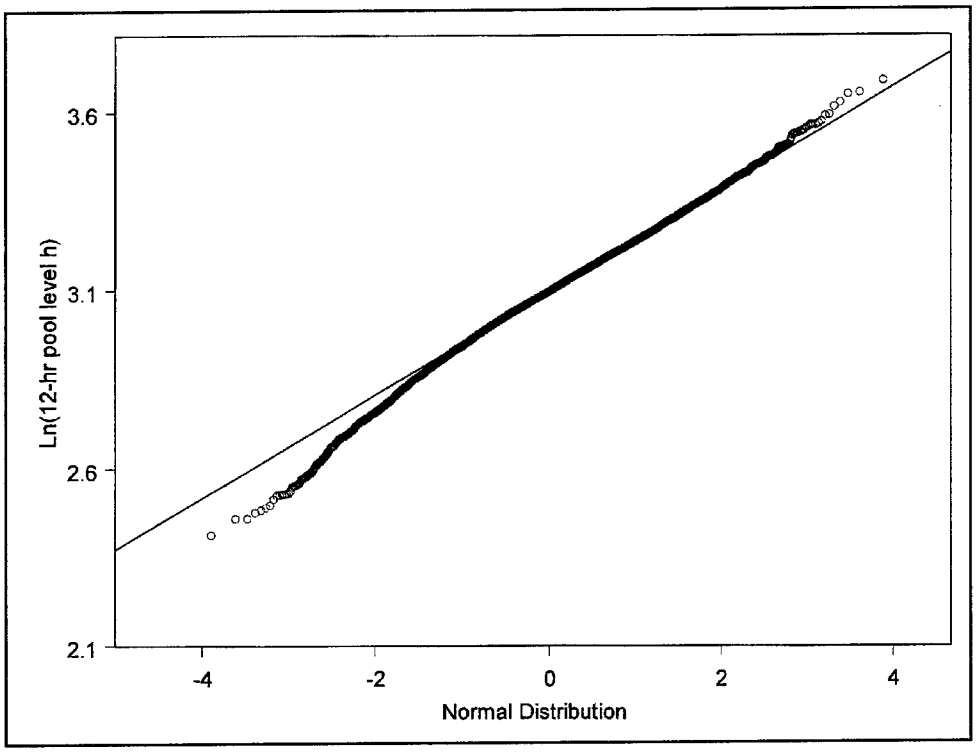

Figure 23. Quantile-quantile plot for $\log_e$ [h(12)] based on 10,000 simulations

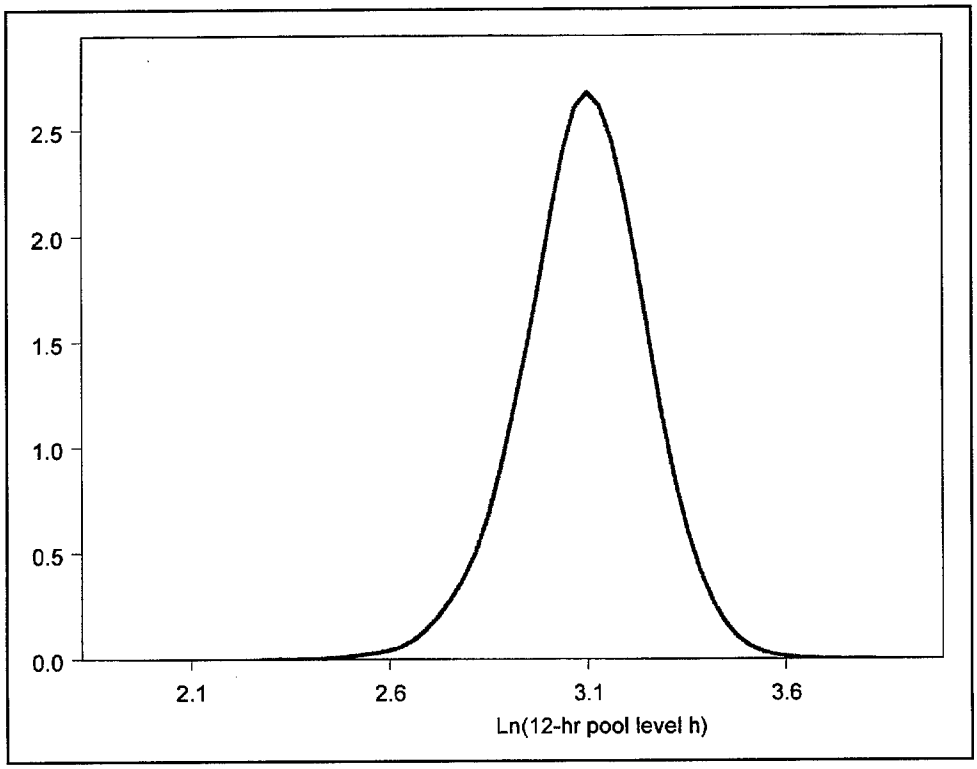

Figure 24. Nonparametric probability density for $\log_e$ [h(12)] based on 10,000 simulations

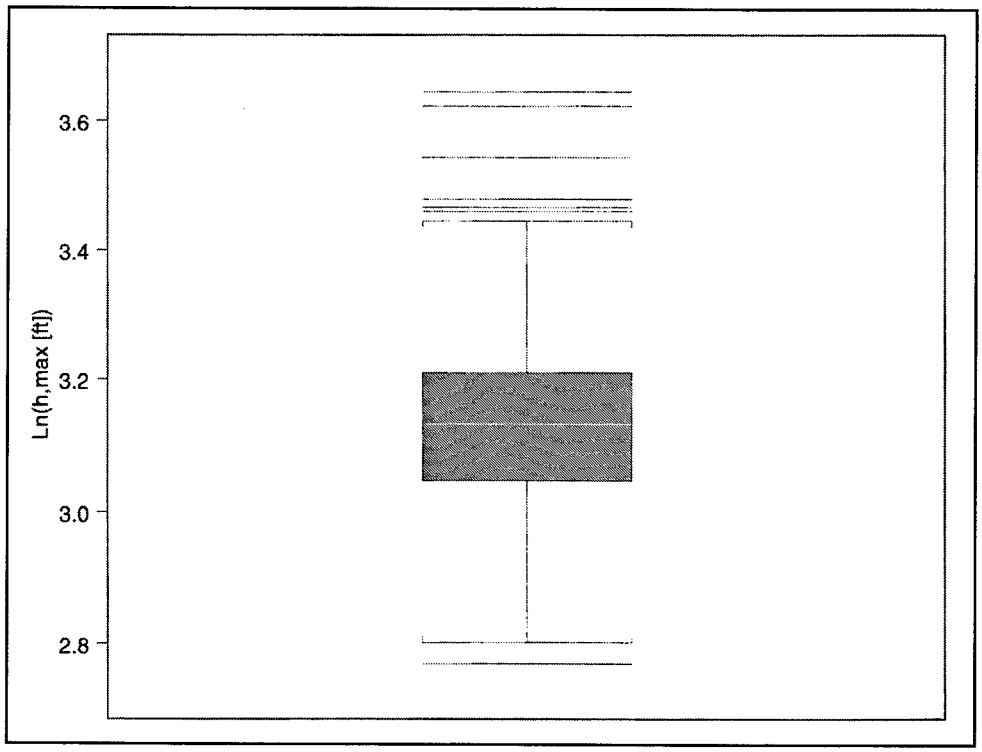

Figure 25. Box plot for $\log_e [h_{,max}]$ based on 1,000 simulations

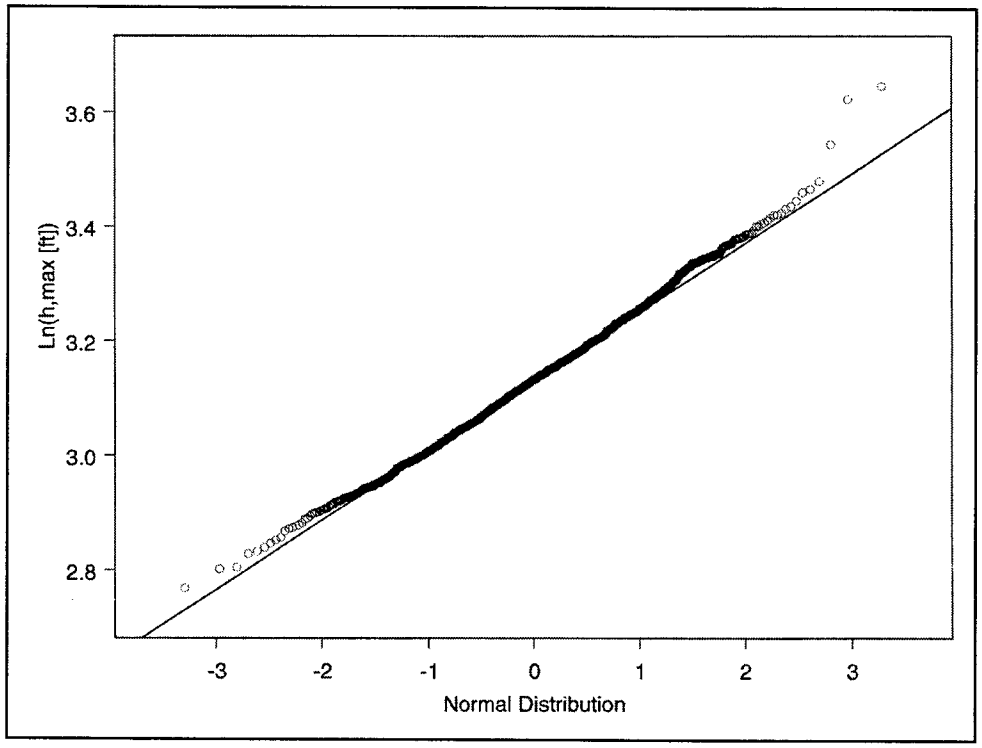

Figure 26. Quantile-quantile plot for $\log_e [h_{,max}]$ based on 1,000 simulations

corresponding quantile-quantile plot that confirms the goodness-of-fit of the log-normal distribution for most of the data (again, a few deviant points are identified at the tails of the distribution). Figure 27 shows the corresponding nonparametric probability density function on the basis of 1,000 simulations.

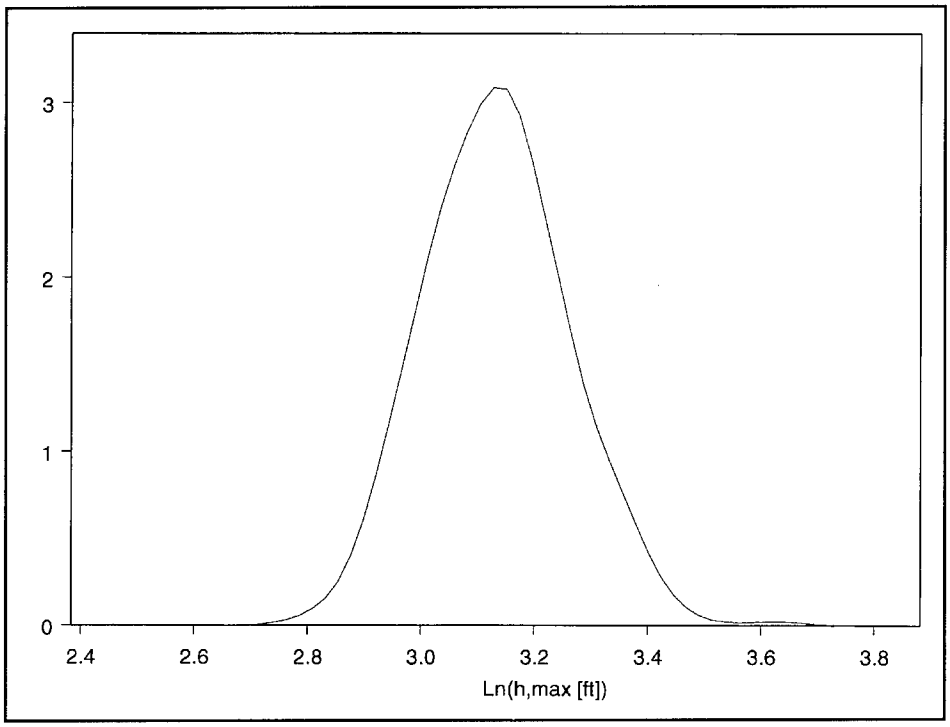

Figure 27. Nonparametric probability density for $\log_e [h_{,max}]$ based on 1,000 simulations

Time to Peak Reservoir Pool

The time ($\check{T}$) to reach the maximum reservoir pool (h,max) is another random variable of interest in the routing process. On the basis of 10,000 simulations, the resultant time for the maximum reservoir pool appears as a cloud of points with no particular pattern. However, upon transformation of both random variables (centering about the mean, followed by scaling down by the corresponding standard deviation), the data are fitted reasonably well by a cubic polynomial. In terms of normalized variables, one obtains:

$$y = -0.19 - 0.7 \cdot x + 0.21 \cdot x^2 - 0.028 \cdot x^3 \qquad (27)$$

where y and x are the normalized time and maximum reservoir pool, respectively. This fit is shown graphically in Figure 28. Notice that the sum of residuals (= 68.8) for this particular set of simulations is satisfactorily small for practical applications. (This sum of residuals is not significantly reduced by increasing the degree of the fitting polynomial up to 10 deg).

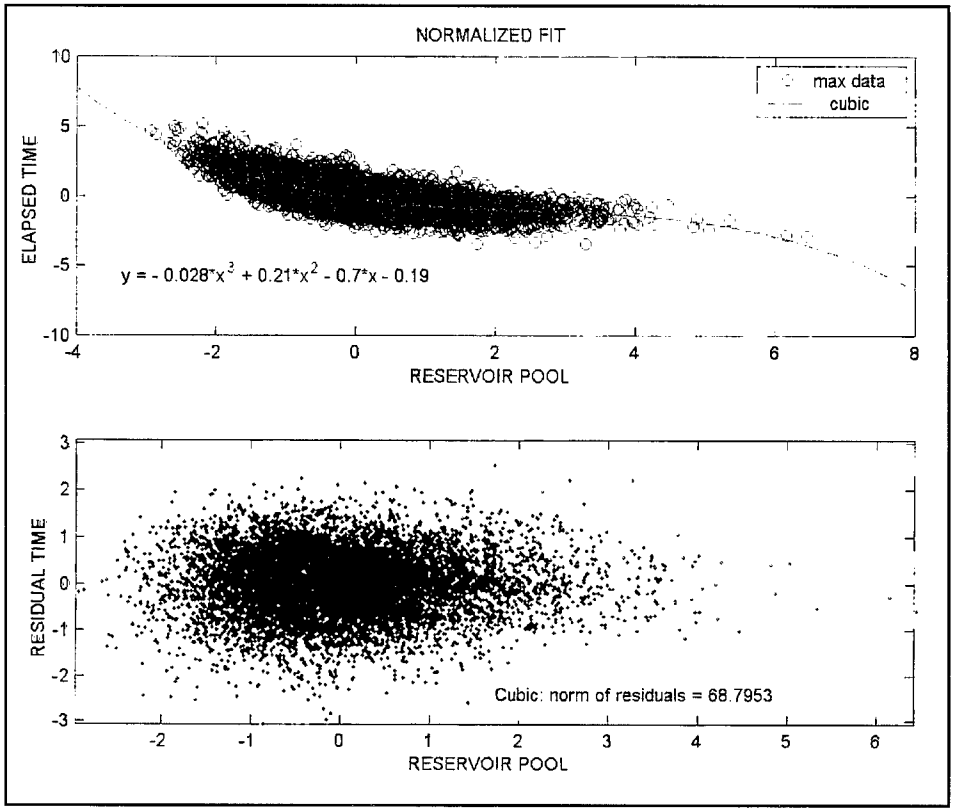

Figure 28. Cubic regression to estimate the time of occurrence of the maximum reservoir pool, $h_{,max}$, based on 10,000 simulations

Noise in the Reservoir

Consider that the bottom of the reservoir may be randomly covered with sediments over time; that our topographical surveys are imperfect, particularly in the vicinity of the boundary of the reservoir; or that the actual values of the regression coefficients α and β for the gradient of reservoir storage with changes in reservoir pool may deviate randomly from the theoretical estimations. The influence of these factors on the reservoir response can be modeled by including a Gaussian noise term in the governing differential equation for the reservoir (Jiang 1998). The result of such formulation is equivalent to adding to the reservoir pool response obtained before (upon solving Equation 19) the contribution to the response from the Gaussian noise term, $\hbar(t)$, which is governed by the following zero-initial condition Itō stochastic differential equation (Larson and Shubert 1979):

$$\frac{d\hbar(t)}{dt} = \frac{\sigma}{G\left[h(t)\right]} \cdot \frac{dW_0(t)}{dt} \tag{28}$$

where

$h(t)$ = total reservoir pool response (including the contribution from the noise)

$dW_0(t)/dt$ = white Gaussian noise

σ = noise intensity

This expression may also be written as the following special case of the Langevin's equation:

$$d\hbar(t) = \frac{\sigma}{G[h(t)]} \cdot dW_0(t) \tag{29}$$

where W_0 is the standard Wiener process.

The solution for this unpredictable noise is given by the following Wiener integral:

$$\hbar(t) = \sigma \cdot \int_0^t \frac{dW_0(\tau)}{G[h(\tau)]} \tag{30}$$

which may be expressed in discrete form for numerical calculations as the following Itō summation:

$$\hbar(t_i) = \sigma \cdot \sum_{t_k=0}^{t_i-\Delta t} \frac{1}{\alpha + \beta \cdot h(t_k)} \cdot \Delta W_0(t_k) \tag{31}$$

where

$\Delta W_0(t_k) = W_0(t_{k+1})$

$W_0(t_k)$ = zero-mean Gaussian process with variance $\Delta t_k = t_{k+1} - t_k = \Delta t$, and

Δt = time-step

The empirical value of the noise intensity, σ, needs to be identified for the specific reservoir under study, and it is arbitrarily taken as σ = 3.5E+4 $ft^3 sec^{-1/2}$ for numerical calculations in this investigation.

Figure 29 shows the mean function for the reservoir pool assumed to be given by the deterministic response hydrograph for the watershed-reservoir-dam system with the input data described in Figure 6. The evolution of the corresponding response random process assumed as log-normally distributed is also shown in Figure 29. Notice that, generally, as time increases along the recession limb, there is less dispersion in the prediction, since the response variances decrease. The pool response to the water-input event with noise in the reservoir is included in the figure, for comparison with the corresponding response without noise. In general, the presence of the noise increases the dispersion of the response random process under consideration. Figure 30 shows the flood hazard curve for the reservoir pool, with and without noise in the reservoir, assuming the response random process to be log-normally distributed. Notice that the noise causes the

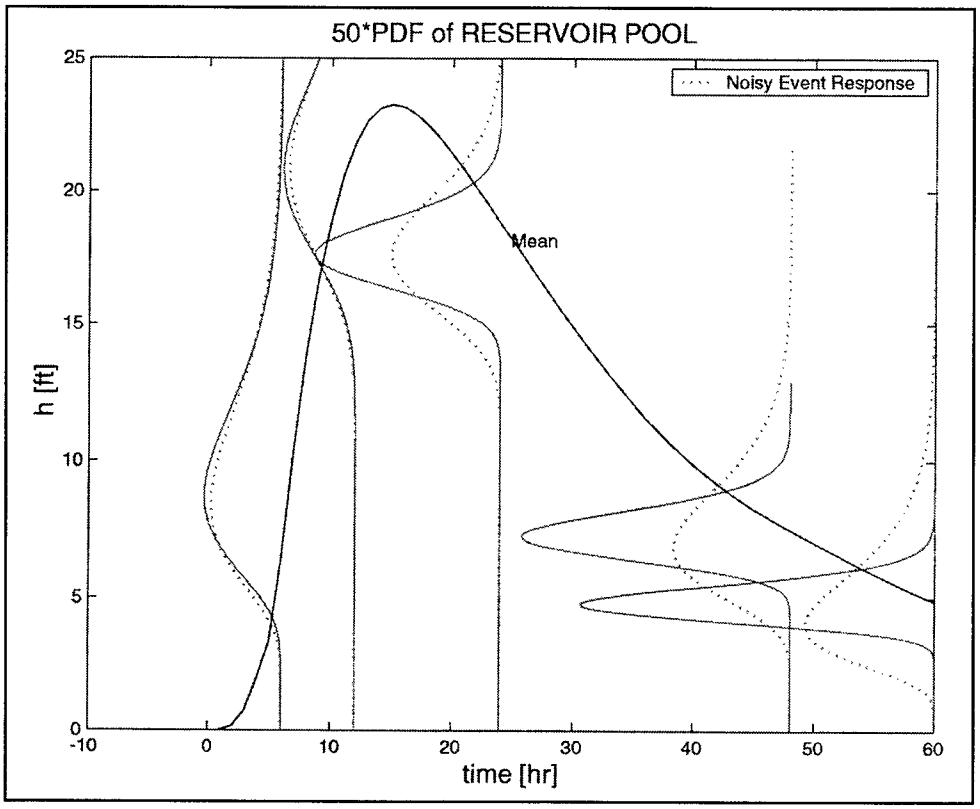

Figure 29. Mean function of the reservoir pool and schematic representation of the random process *h(t)*, assumed log-normal, with and without noise in the reservoir (for clarity, probability density functions appear amplified by a factor of 50)

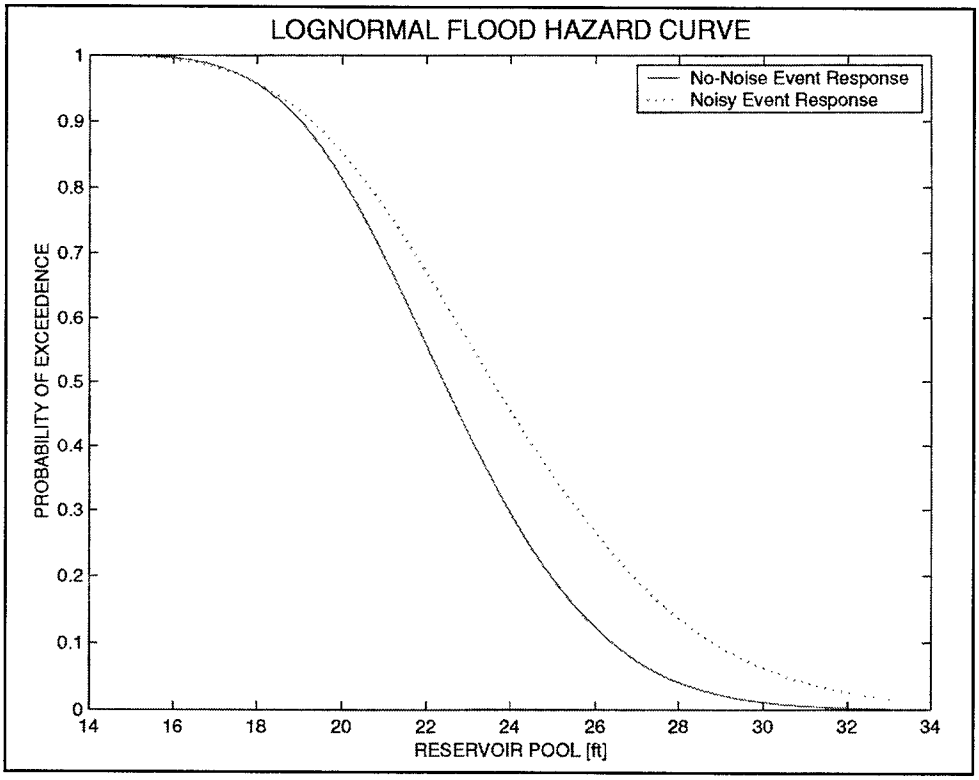

Figure 30. Flood hazard curve for the random process *h(t)*, assumed log-normal, with and without noise in the reservoir

hazard to increase substantially. For example, given that the crest of the nonoverflow section is, say, 30 ft above the level of the spillway crest, the probability of overtopping turns out to be 6.2 percent for a noisy reservoir, as compared to 2.4 percent for an ideal reservoir. Figure 31 represents a parallel development for the flood hazard curve, assuming that the reservoir pool response process is normally distributed. Now the probability of overtopping is 4.5 percent for a noisy reservoir, as compared to 0.4 percent for an ideal reservoir.

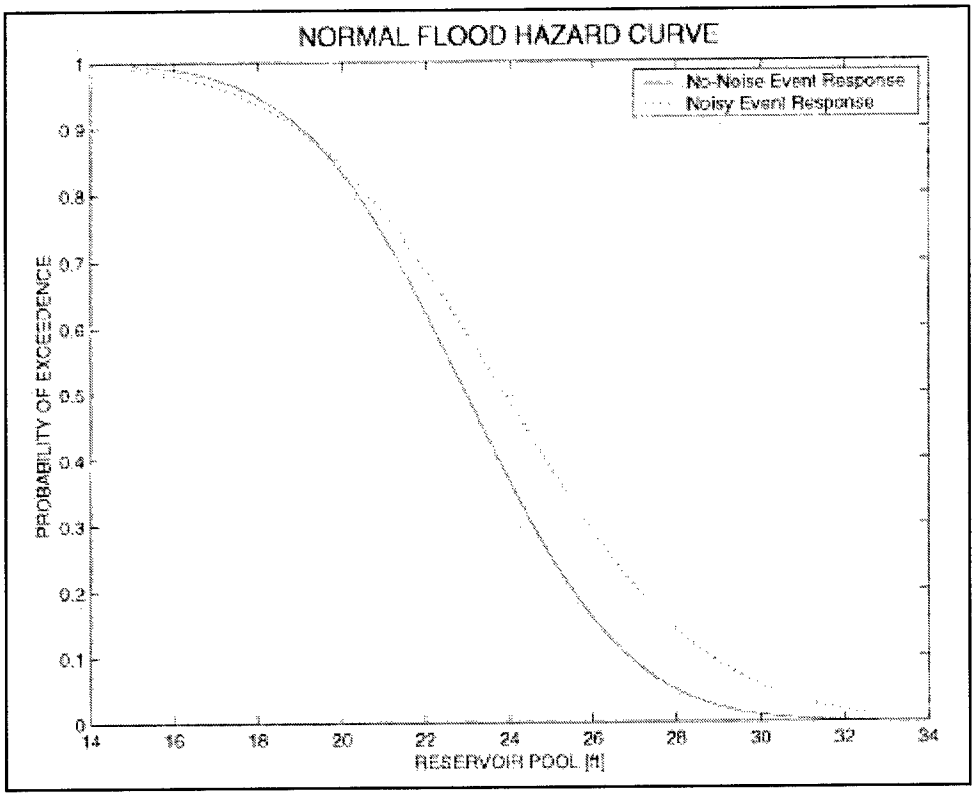

Figure 31. Flood hazard curve for the random process h(t), assumed normal, with and without noise in the reservoir

In general, the magnitude of the hazard is increased when the response processes as taken as log-normally distributed, as compared to the results with the normal assumption. The log-normal assumption for the response process has been proved in this investigation to be applicable to the probabilistic simulation of routing of a water-input event through a watershed-reservoir-dam system. Therefore, the use of the log-normal distribution is recommended for practical applications to real systems in the field.

5 Conclusions

The following conclusions are derived from this investigation:

a. A rational theoretical model has been developed to represent the routing of a water-input event through a watershed-reservoir-dam system and to assess its response in terms of the inflow design flood into the reservoir and the resulting reservoir pool.

b. Both deterministic and probabilistic implementations of the model allow ready computational analysis, useful for both design and for situational assessment.

c. System response random processes are best modeled as log-normally distributed.

d. Noise in the reservoir component is easily included in the probabilistic formulation of the model and has an important influence in the magnitude of the resulting hazard. An accurate assessment of the noise intensity may prove difficult in practice, but realistic reliability assessments can be conducted using bounds on the noise intensity.

e. The model provides direct evaluation of the probability of overtopping in a given flood scenario and provides the fundamental hazard curve for complete risk analysis of the dam structure, including the possible sliding, overstressing, and overturning modes of failure.

References

de Béjar, L. A. (1999). "Fragility analysis of concrete gravity dam safety under flood." *Proceedings of ASDSO Dam Safety '99.* St. Louis, MO.

Benjamin, J. R., and Cornell, C. A. (1970). *Probability, statistics, and decision for civil engineers.* McGraw-Hill, New York, NY.

Dingman, S. L. (1994). *Physical hydrology.* Macmillan, New York, NY.

Ellingwood, B. R. (1995). "Engineering reliability and risk analysis for water resources investments: Role of structural degradation in time-dependent reliability analysis," Contract Report ITL-95-3, U.S. Army Engineer Waterways Experiment Station, Vicksburg, MS.

Hoggan, D. H. (1997). *Computer-assisted hydrology and hydraulics.* 2nd ed., McGraw-Hill, New York, NY.

Jiang, S. (1998). "Application of stochastic differential equations in risk assessment for flood releases," *J. Hydrological Sciences* 43(3), 349-360.

Larson, H. J., and Shubert, B. O. (1979). *Probabilistic methods in engineering sciences. Vol. II: Random noise, signals, and dynamic systems.* Wiley, New York, NY.

MathSoft. (1999). *S-plus 2000 modern statistics and advanced graphics.* Seattle, WA.

Miller, D. L., and Clark, R. A. (1960). "Flood studies." *Design of small dams.* 1st ed., U.S. Department of the Interior, Bureau of Reclamation, Denver, CO.

Olson, R. M. (1961). *Engineering fluid mechanics.* International Textbook, Scranton, PA.

Street, R. L., Watters, G. Z., and Vennard, J. K. (1996). *Elementary fluid mechanics.* 7th ed., Wiley, New York, NY.

The MathWorks. (2000). *Matlab 6.0 user's manual.* Natick, MA.

U.S. Bureau of Reclamation. (1976). "Design of gravity dams; Appendix G: Inflow design flood studies," U.S. Department of the Interior, Denver, CO.

_____. (1977). "Design of arch dams; Appendix L: Inflow design flood studies," U.S. Department of the Interior, Denver, CO.

REPORT DOCUMENTATION PAGE

Form Approved
OMB No. 0704-0188

1. REPORT DATE *(DD-MM-YYYY)*	2. REPORT TYPE	3. DATES COVERED *(From - To)*
August 2001	Final report	

4. TITLE AND SUBTITLE

Convex Watershed-Reservoir Model for Risk Assessment of Spillways and Nonoverflow Dam Monoliths Subjected to Flood Hazard

5a. CONTRACT NUMBER

5b. GRANT NUMBER

5c. PROGRAM ELEMENT NUMBER

6. AUTHOR(S)

Luis A. de Béjar

5d. PROJECT NUMBER

5e. TASK NUMBER

5f. WORK UNIT NUMBER

7. PERFORMING ORGANIZATION NAME(S) AND ADDRESS(ES)

U.S. Army Engineer Research and
Development Center
Geotechnical and Structures Laboratory
3909 Halls Ferry Road
Vicksburg, MS 39180-6199

8. PERFORMING ORGANIZATION REPORT NUMBER

ERDC/GSL TR-01-8

9. SPONSORING / MONITORING AGENCY NAME(S) AND ADDRESS(ES)

U.S. Army Corps of Engineers
Washington, DC 20314-1000

10. SPONSOR/MONITOR'S ACRONYM(S)

11. SPONSOR/MONITOR'S REPORT NUMBER(S)

12. DISTRIBUTION / AVAILABILITY STATEMENT

Approved for public release; distribution is unlimited.

13. SUPPLEMENTARY NOTES

14. ABSTRACT

This investigation introduces a convex model to describe the response of watershed-reservoir-dam systems to water-input events and to build corresponding flood hazard curves in support of evaluations of risk for dam safety.

The following conclusions are derived from this investigation:

a. A rational theoretical model has been developed to represent the routing of a water-input event through a watershed-reservoir-dam system and to assess its response in terms of the inflow design flood into the reservoir and the resulting reservoir pool.

b. Both deterministic and probabilistic implementations of the model allow ready computational analysis, useful for both design and for situational assessment.

c. System response random processes are best modeled as log-normally distributed.

d. Noise in the reservoir component is easily included in the probabilistic formulation of the model and has an important influence in the magnitude of the resulting hazard. An accurate assessment of the noise intensity may prove difficult in practice, but realistic reliability assessments can be conducted using bounds on the noise intensity.

(Continued)

15. SUBJECT TERMS

Flood hazard
Probabilistic models of spillways
Risk assessment
Watershed-reservoir model

16. SECURITY CLASSIFICATION OF:			17. LIMITATION OF ABSTRACT	18. NUMBER OF PAGES	19a. NAME OF RESPONSIBLE PERSON
a. REPORT	b. ABSTRACT	c. THIS PAGE			19b. TELEPHONE NUMBER *(include area code)*
UNCLASSIFIED	UNCLASSIFIED	UNCLASSIFIED		42	

14. (Concluded).

e. The model provides direct evaluation of the probability of overtopping in a given flood scenario and provides the fundamental hazard curve for complete risk analysis of the dam structure, including the possible sliding, overstressing, and overturning modes of failure.